Causes of Infection and Disease Progression of *Hematodinium sp.* in the Tanner crab, *Chionoecetes bairdi*

Aspen Elizabeth Coyle

A thesis
submitted in partial fulfillment of the
requirements for the degree of

Master of Science

University of Washington
2024

Committee:
Steven Roberts
Chelsea Wood

Program Authorized to Offer Degree:
School of Aquatic and Fishery Sciences

Abstract

Causes of Infection and Disease Progression of *Hematodinium sp.* in the Tanner crab,
Chionoecetes bairdi

Aspen Elizabeth Coyle

Chair of the Supervisory Committee:
Steven Roberts
School of Aquatic and Fishery Sciences

In the past several decades, parasites of the genus *Hematodinium* have become prevalent in crustaceans around the globe. One such host is the Tanner crab (*Chionoecetes bairdi*), which supports a number of commercially and culturally valuable fisheries in the North Pacific. This thesis explores the host-parasite relationship between *C. bairdi* and *Hematodinium* sp. through two avenues. The first was an analysis of gene expression, in which individual crabs were captured, their infection status was checked, and they were exposed to one of three temperatures - elevated, decreased, and control. Throughout the 17-day experiment, hemolymph was drawn and sequenced for gene expression. Differences in gene expression for both host and parasite were then analyzed, and a number of genes in both host and parasite were identified as linked to temperature response. Numerous parasite expression pathways changed over the course of the experiment, including changes in RNA processing and microtubule development. The second avenue of analysis utilized generalized linear mixed models to investigate a long-term survey dataset from southeast Alaskan crab surveys, with the goal of determining the association between infection status and a variety of biological and environmental factors. A number of factors were found to be correlated to infection status. Among them: females were more likely to be infected than males, immature crab were more likely to be infected than mature individuals, recently-molted crabs were more likely to be infected, and larger crabs were more likely to be infected. Together, these findings improve our understanding of the relationship between *C. bairdi* and *Hematodinium*. They provide a window into the internal host-parasite dynamics and how temperature and time alter gene expression. They also demonstrate that infection rates vary substantially within subsets of the host population, and indicate those subset-specific impacts should be considered when analyzing the ramifications of outbreaks.

TABLE OF CONTENTS

List of Tables and Figures....................ii

Chapter 1....................1

  1.1 Introduction....................1

  1.2 Methods....................4

  1.3 Results....................10

  1.4 Discussion....................20

Chapter 2....................25

  2.1 Introduction....................25

  2.2 Methods....................27

  2.3 Results....................32

  2.4 Discussion....................38

References....................42

LIST OF TABLES AND FIGURES

Figure 1. Experimental design for Chapter 1 5

Table 1. Differential expression comparisons 13

Figure 2. Parasite functional enrichment over course of experiment 15

Figure 3. Heatmap of *C. bairdi* gene expression clusters 17

Figure 4. Heatmap examining impact of change in parasite burden on host expression 18

Figure 5. Heatmap of parasite gene expression clusters 19

Figure 6. Functional enrichment of parasite gene module 20

Figure 7. Survey locations for Chapter 2 29

Figure 8. Estimated coefficients in the general model 33

Figure 9. Relationships between variables and BCS status 34

Figure 10. Estimated coefficients in the sex-specific models 36

Figure 11. Relationships between sex-specific variables and BCS status 37

ACKNOWLEDGMENTS

First, I would like to thank my advisor, Dr. Steven Roberts, for all his help, his patience, and his understanding, and for taking a chance on me in the first place. Literally everything I know about bioinformatics comes, in some way, from his guidance.

I would like to thank Dr. Chelsea Wood. Her dedication, knowledge, and passion is a constant inspiration, and I am honored to have her on my committee.

I would like to thank Zach, Chris, Celeste, Yaamini, Grace, Kathleen, and the rest of the members of the Roberts lab. Thanks for being such a supportive and warm group. And extra thanks to Sam White for being an endless font of knowledge and advice and help.

I would like to thank José Guzman for being an incredible source of support and advice, as well as being just an absolute joy to TA for.

I would like to thank Grace Crandall and Pam Jensen - half of this thesis is based entirely on data they collected, and I am eternally grateful for their hard work

I would like to thank the members of the Alaska Department of Fish and Game crab teams - both in Southeast, who provided so much valuable data, and in Kodiak, who made me into a scientist who could begin to tackle this work.

Finally, I would like to thank SAFS. For providing me with the funding to carry out this research, for helping me grow as a scientist, for supporting me through some fairly massive life changes, and for just being a wonderful community.

DEDICATION

To Mom, Dad, Katie, Lia, Zoe, Matthew, Josie, Piper, Dria, and Tay. Couldn’t have done this without you.

And to Donut, Steph, Maeve, Bonnie, Amber, and the whole trans community.
I love you all dearly

CHAPTER 1

1.1 INTRODUCTION

Parasites impact their hosts in a wide variety of ways, and can thus play a number of ecological roles. In addition to altering the behavior and physiology of the host, parasites can shift competitive balance within the host. This can make the host more susceptible to additional infections, but can also reduce susceptibility. Humans infected by parasitic helminths, for example, are less prone to infection by Giardia (Martin et al. 2013). Parasites can also shift community composition, as has been observed in Britain, where native red squirrels are declining partly due to a virus carried by invasive and immune grey squirrels (Tompkins et al. 2003). Finally, parasites can change the composition of ecosystems. After the eradication of rinderpest in Africa the population of wildebeest exploded. The increased grazing sharply reduced fires, which resulted in increased tree cover (Holdo et al. 2009). Clearly, understanding parasites - particularly highly pathogenic ones with common hosts - can be crucial to understanding the dynamics of an ecosystem (Wood & Johnson 2015).

The parasitic dinoflagellate *Hematodinium* is a host generalist, infecting over 40 species of crab, shrimp, and lobster, including many important species for commercial fisheries and aquaculture (Li et al. 2021). Outbreaks have occurred globally, often causing major economic damage (Li et al. 2021). Prior to 1985, only six studies described *Hematodinium* infections, all of which were confined to France and the east coast of the United States (Morado et al. 2011). In the following decades, *Hematodinium* was observed throughout the North Atlantic, North Pacific, China, and Australia (Small 2012). Today, new hosts and ranges are regularly reported (Li et al. 2021; Ryazanova et al. 2021). In some host-parasite systems its prevalence is correlated with a warming climate, while in others no such correlation appears (Morado et al. 2011). Within many hosts, *Hematodinium* prevalence varies seasonally (Eaton et al. 1991; Messick 1994; Hamilton et al. 2009; Davies et al. 2019).

Hematodinium has an exceptionally complex life cycle, with in vitro experiments identifying at least 10 distinct stages (Li et al. 2011). Heavily infected host individuals often produce large numbers of dinospores (Li et al. 2010), which are presumed to be the infective stage. Infections occur predominantly through waterborne transmission, though the specific method of entry into the host is unknown (Shields et al. 2017). In numerous host species, including *Chionoecetes* spp., infection is closely associated with molting (Shields et al. 2007, Messick 1994; Meyers et al. 1990), with speculation that small cracks in the integument of a freshly molted crab allow entry of *Hematodinium* dinospores (Meyers et al. 1990). Upon entering the host, the dinoflagellate proliferates within the hemolymph and organs, eventually resulting in respiratory dysfunction, extreme lethargy, and mortality (Stentiford & Shields 2005).

Distributed along the continental shelf from Oregon to the southern Bering Sea, the Tanner crab (*Chionoecetes bairdi*) has substantial economic and societal importance (Heller-Shipley et al. 2021). *C. bairdi* is often infected by an undescribed *Hematodinium* species (Jensen et al. 2010). Infection rates vary seasonally, peaking in the late summer and early fall (Love et al. 1993). Summer prevalence can be quite high, with infection rates over 50% in portions of *C. bairdi*'s range (Bednarski et al. 2011). The progress from initial infection to mortality is slow, and takes place over a minimum of several months (Love et al. 1993). Heavy infections of *Hematodinium* sp. are marked by milky white hemolymph, an opaque white or pink coloration, and bitter, unpalatable flesh (Meyers et al. 1990).

The long duration between infection and symptoms, elaborate life cycle of *Hematodinium*, and challenges of experimentally inducing infection have hampered efforts to investigate this complex host–parasite system. However, the need to obtain answers is growing more critical. Infection rates are climbing in *C. bairdi*, particularly in the Bering Sea portion of its range, as are infection rates in its close relative *C. opilio* (NOAA 2020, unpublished data). Furthermore, much of the range of *C. bairdi* has recently been struck by anomalous heat events (Di Lorenzo & Mantua 2016, Cheung et al. 2020). Marine heatwaves are projected to increase in frequency and intensity due to anthropogenic warming (IPCC 2019). Understanding the environmental drivers of infection by *Hematodinium* is critical to proper management of this valuable fishery and for its preservation for years to come.

Previous research has characterized gene expression patterns in *C. bairdi* infected with *Hematodinium* at various temperatures (Crandall et al. 2021). However, that work has focused on examining pooled libraries of hosts, rather than tracking the response of individual crabs under different temperature regimes, and was not able to examine gene expression of *Hematodinium*. Transcriptomics provides a powerful tool to examine response of both host and parasite to changing environmental conditions. The purpose of this study was to improve our understanding of the dynamics within this host–parasite system by investigating the response of both *Hematodinium* sp. and infected *C. bairdi* to changes in temperature, and to track the progression of disease within infected crab. Specifically, we used transcriptomics to uncover overall changes in gene expression and stress response within both host and parasite, along with an examination of immune response.

1.2 METHODS

1.2.1 *Experimental Design*

Male *C. bairdi* were collected with pots (n = 400) from Stephens Passage in southeastern Alaska in October 2017, a location with a reliably high prevalence of *Hematodinium* infection (Bednarski et al. 2011; ADF&G, unpublished data). Crabs were transported to the Ted Stevens Marine Research Institute in Juneau, AK and held in a flow-through system at the bottom temperature of Stephens Passage at time of capture, 7.5°C, for a 9-day acclimation period. At the end of this period, crabs that did not appear to have completely recovered from capture stress were discarded. The end of the acclimation period and beginning of the experiment is henceforth noted as Day 0.

A hemolymph sample (0.2ml) was drawn from the 179 remaining crabs selected and preserved in RNAlater (1200 µl). Crabs were divided into three groups, with 60 crabs in each experimental group and 59 in the control temperature treatment group. The control temperature group continued to be held at 7.5°C, while water temperature within the elevated-temperature and decreased-temperature treatment group was gradually changed over a two-day period to 10°C and 4°C, respectively. A second hemolymph sample was drawn from the 177 surviving crabs and preserved in RNAlater. Temperatures were maintained for an additional 15 days, for a total experimental duration of 17 days (**Figure 1**). The remaining crabs then had additional hemolymph samples withdrawn and preserved in RNAlater.

The elevated-temperature treatment group saw a mass mortality event, with 58 of the 60 of crabs dying prior to the end of the experiment. Over the same period, there were eight mortalities within the decreased-temperature treatment group, and three mortalities within the control temperature group. Hemolymph samples were taken from the two surviving crabs in the elevated-temperature treatment group, but their RNA yield was not sufficient for sequencing.

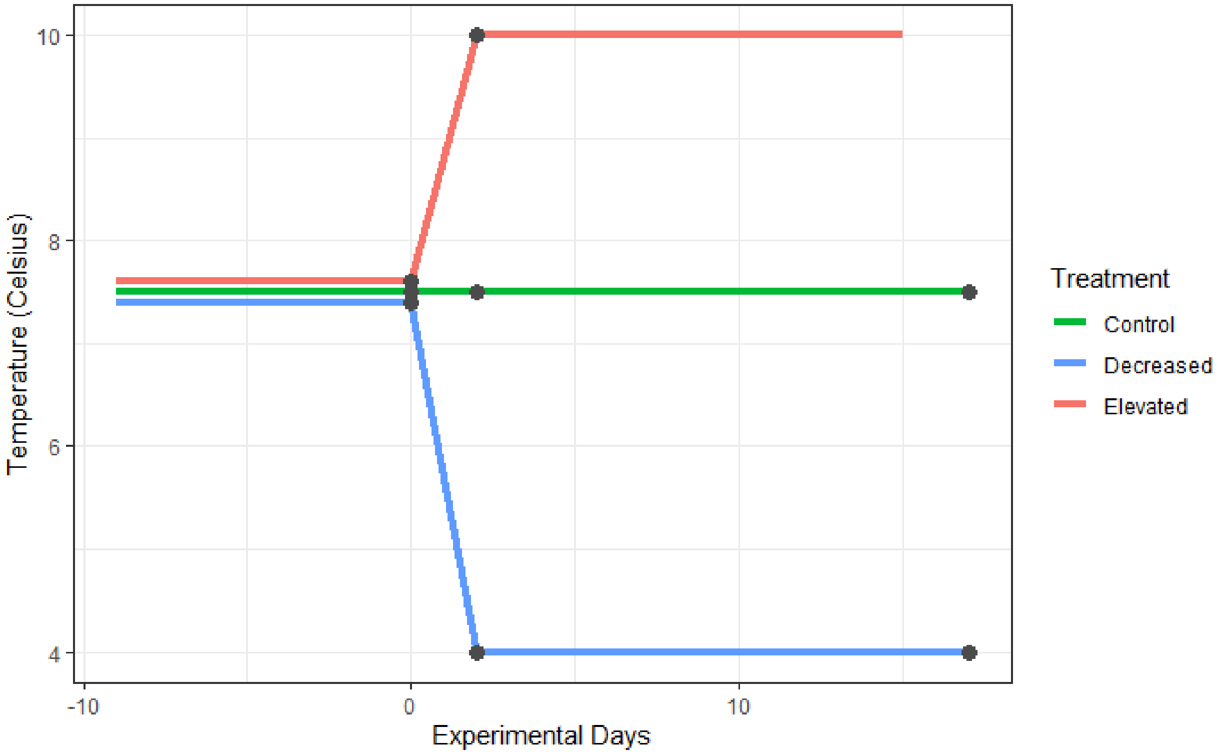

Figure 1. Diagram of temperature of each treatment group over the course of the experiment. Days are indexed from zero, beginning at the initiation of temperature changes for experimental groups. Three RNA samples were taken from each treatment group on days 0, 2, and 17, marked with black dots, and sequenced. Due to a mortality event, no samples with sufficiently high RNA yields were taken from elevated-temperature crabs on day 17.

1.2.2 *Infection Status Assessment*

Hemolymph samples from the start and (if available) end of the experiment had DNA extracted, subjected to qPCR following established protocol for *Hematodinium* sp. (Crosson 2011) to determine the level of *Hematodinium* sp. infection. Samples were tested in duplicate.

1.2.3 *RNAseq*

A total of nine crabs, three from each temperature regime, were selected based on RNA yields. As determined by qPCR, all nine were infected with *Hematodinium*. Total RNA was extracted from all hemolymph samples of these crabs using Quick DNA/RNA Microprep Plus Kit (Zymo Research) according to the manufacturer's protocol. This created a total of 24 samples, with samples from Days 0, 2, and 17 the control and decreased-temperature treatment crabs. Due to the mortality event, the final samples were not available for elevated-temperature treatment crabs. All samples were sent to Genewiz, Inc. for library construction and RNAseq. Samples were sequenced as paired end (100bp and 150bp) on HiSeq4000 (Illumina, Inc.) sequencers.

To increase transcriptome completeness, 11 additional sequencing samples were created by pooling 112 hemolymph samples from 87 more crabs based on treatment, sampling day, and infection status (Supplemental Table 1). These samples were sent to the Northwest Genomics Center at Foege Hall at the University of Washington for RNAseq and library construction. Samples were sequenced as paired end (100bp and 150bp) on NovaSeq (Illumina, Inc.) sequencers.

1.2.4 *Transcriptome Assembly and Annotation*

Raw sequence data were assessed using FastQC (v0.11.8; Andrews 2010) and MultiQC (v1.6; Ewels et al. 2016) pre- and post-trimming. Data were quality trimmed using fastp (v0.20.0) (Chen et al. 2018). Trimmed reads were used for all subsequent analyses. All raw sequencing data is available in the NCBI Sequence Read Archive (SRR11548643-SRR11548677).

A transcriptome was *de novo* assembled from all individual and pooled libraries using Trinity (v2.9.0; Grabherr et al. 2011; Haas et al. 2013). This is hereafter referred to as the complete transcriptome. The complete transcriptome was assessed with BUSCO (v3.0.2; Simão et al. 2015; Waterhouse et al. 2018) using the metazoa_odb9 database, Augustus (v3.3.2; Stanke and Waack 2003; Stanke et al. 2008) with species set as fly, and hmmer (v3.2.1; hmmer.org). The transcriptome was then annotated and GO terms were obtained using DIAMOND BLASTx against the UniProtKB/Swiss-Prot database (downloaded 2021-02-09).

To examine host expression, a crab-specific transcriptome was created. To identify crab-specific sequencing reads, sequencing reads from all individual and pooled libraries were compared to the publicly available proteome (NCBI Acc: GCA_016584305.1) of a congener, *Chionoecetes opilio* (snow crab) using DIAMOND BLASTx (v0.9.29; Buchfink et al. 2015). Reads identified as matching (e-value <= 1E-04) *C. opilio* were extracted from the FastQs using seqkit (v.0.15.0; Shen et al. 2016). These crab specific reads were *de novo* assembled using Trinity (v2.12.0; Grabherr et al. 2011; Haas et al. 2013). This assembly is hereafter referred to as the *C. bairdi* transcriptome. The *C. bairdi* transcriptome was assessed for completeness with BUSCO (v3.0.2; Simão et al. 2015; Waterhouse et al. 2018) using the metazoa_odb9 database, Augustus (v3.3.2; Stanke and Waack 2003; Stanke et al. 2008) with species set as fly, and hmmer (v3.2.1; hmmer.org). The transcriptome was then annotated and GO terms were obtained using DIAMOND BLASTx against the UniProtKB/Swiss-Prot database (downloaded 2021-02-09). In another publication originating from these data, pooled libraries were aligned to the crab-specific transcriptome and analyzed for differential expression between treatment groups, as were all libraries from one of the nine crabs in this study (Crandall et al. 2022). However, analysis in that publication did not continue further to examine individual host response or non-host response.

A third transcriptome was created to examine expression in *Hematodinium* sp. Sequences from all individual and pooled libraries were taxonomically categorized with a combination of DIAMOND BLASTx (0.9.26; Buchfink et al. 2015) and MEGAN6 (6.18.3; (Huson et al. 2016)). DIAMOND BLASTx was run against NCBI nr database (downloaded 2019-09-25). The resulting DAA files were converted to RMA6 files for importing into MEGAN6 with the daa2rma utility, using the following MEGAN6 mapping files: prot_acc2tax-Jul2019X1.abin, acc2interpro-Jul2019X.abin, acc2eggnog-Jul2019X.abin. All sequencing reads categorized within and below the phylum Alveolata were identified using MEGAN6 (v6.18.3; Huson et al. 2016). Subsequently, these reads were extracted from the FastQ files using seqtk (Shen et al. 2016) and *de novo* assembled using Trinity (v2.12.0; Grabherr et al. 2011; Haas et al. 2013). Since all crabs were confirmed to be infected with *Hematodinium*, and no other Alveolata parasites of *C. bairdi* have been identified, this transcriptome likely contains only *Hematodinium* sequences. However, as the presence of other Alveolata species could not be ruled out, this is hereafter referred to as the Alveolata transcriptome. The Alveolata transcriptome was assessed for completeness with BUSCO (v3.0.2; Simão et al. 2015; Waterhouse et al. 2018) using the metazoa_odb9 database, Augustus (v3.3.2; Stanke and Waack 2003; Stanke et al. 2008) with species set as fly, and hmmer (v3.2.1; hmmer.org). The transcriptome was then annotated and GO terms were obtained using DIAMOND BLASTx against the UniProtKB/Swiss-Prot database (downloaded 2021-02-09).

This work was facilitated through the use of advanced computational, storage, and networking infrastructure provided by the Hyak supercomputer system at the University of Washington. Links to the transcriptome assemblies and files are available in Supplemental Table 2.

1.2.5 *Differential Expression Analysis*

Quality trimmed libraries of individual crabs were pseudo-aligned to each of the three transcriptomes (complete, *C. bairdi*, and Alveolata) using kallisto (Bray et al. 2016). Two different approaches were then used to examine differential expression.

To evaluate the impact of changes in temperature on expression, the R package DESeq2 (Love et al. 2014) was used to perform pairwise comparisons. Pairwise comparisons were performed within each temperature regime, comparing expression prior to, and following, the initiation of temperature changes. Abundance matrices were produced using the Trinity (v2.12.0; Grabherr et al. 2011; Haas et al. 2013). Differentially expressed contigs, along with their accompanying accession IDs, were obtained for each comparison (**Table 1**).

In addition to pairwise comparisons within temperature regimes, a clustering approach was used to enable comparisons between treatment groups and examine correlation in expression to each variable. The R package WGCNA was used (Langfelder & Horvath 2008), which clusters contigs into eigengenes based on expression pattern and then calculates correlation between eigengene modules and experimental variables. Categorical variables were binarized, and a signed network was used. This analysis was performed once with all samples, and then again with only samples from crabs that did not die prior to the end of the experiment. This latter analysis included an examination of change in *Hematodinium* infection level over the 17-day experimental period.

1.2.6 Functional Enrichment

Gene ontology (GO) terms were obtained by cross-referencing the accession IDs of each contig with the Gene Ontology database. For differential expression analysis using pairwise comparisons, the log2-fold changes were extracted from the DESeq2 output and paired with GO terms as input for GO-MWU (Wright et al. 2015), which performs a Mann-Whitney U test and utilizes adaptive clustering to examine gene ontology term enrichment.

For WGCNA analyses performed with eigengene clustering, all modules with a significant correlation to a sample trait were examined, and if the significance appeared to be due to correlation to libraries from a single crab, the module was discarded. For all remaining significant modules, the module membership (kME) of its contigs was extracted, and functional enrichment of the module was analyzed using GO-MWU. This procedure was followed twice, once with all samples and once with only control and decreased-temperature treatment samples. The latter specifically examined change in *Hematodinium* infection level over time, as only one time point for *Hematodinium* infection level was available for the elevated-temperature treatment group.

1.3 RESULTS

1.3.1 *Mortality and Hematodinium Detection*

Analysis with qPCR revealed *Hematodinium* infections were present in all crabs. Quantities of *Hematodinium* DNA were compared over the course of the experiment in control and decreased-temperature treatment groups. In four of the six crabs, *Hematodinium* infection intensity decreased, and in three it decreased by at least two orders of magnitude (Supplemental Table 3).

C. bairdi transcriptome

Assembly of quality trimmed and crab-specific reads into a transcriptome produced 88,302 consensus sequences (Roberts, Coyle, & White 2022). A comparison against the

UniProtKB/Swiss-Prot database resulted in 30,094 annotated contigs. Additional assembly statistics are in Supplemental Table 4.

Alveolata transcriptome

Assembly of quality trimmed reads within the phylum Alveolata into a transcriptome yielded 6,176 consensus sequences (Roberts, Coyle, & White 2022). Comparison against the UniProt/Swiss-Prot database produced 3,889 annotated contigs. Additional assembly statistics are in Supplemental Table 4.

1.3.2 *Immune Gene Characterization*

C. bairdi

A number of genes within the *C. bairdi* transcriptome (n = 49) were associated with immune function (GO:0006955). Many were members of the cathepsin family, with cathepsins C, J, L, S, U, V, and W present. Cathepsin L was particularly broadly expressed, with seven distinct genes coding for cathepsin and procathepsin L. Procathepsin L was differentially expressed in the elevated-temperature treatment group over days 0 and 2. Multiple types of MAPKs (mitogen-activated protein kinases) were also present within the transcriptome, including two p38 MAPKs and one MAP4K. MAPKs are part of the IMD (immune deficiency) pathway, a notable component of the crustacean immune system. Several other genes associated with the IMD pathway were observed, including the transcription factor Relish and the kinase inhibitor IκK. NFIL3, a nuclear factor with a role in regulating Relish expression in similar systems, was also present.

Other immune-linked genes observed were Transcription Activator Protein-1 (TF AP-1) and Granzyme A. TF AP-1 acts as an immune system regulator within other crab species, along with a potential role as an osmoregulator (Wang et al. 2018). Little research on the role of Granzyme A in invertebrates has been performed, but in vertebrates it has a cytotoxic role against intracellular pathogens.

Hematodinium

Within the Alveolata transcriptome, four genes were linked to immune function. All four of these were cysteine proteases, which can function in blood cell degradation and invasion, surface proteins processing, and cell egress for intracellular parasites (Verma et al. 2016). Three of the four were cathepsins, including both procathepsin and cathepsin L.

1.3.3 *Differential Expression*

Comparisons within the control temperature treatment group provided context for the frequency of differentially expressed (padj < 0.05) contigs (DE Contigs) expected without a temperature change. Simultaneously, they examined expression over the course of an infection. Comparisons between Day 0 and Day 2 in an experimental group examined short-term changes to a temperature shift, while comparisons between Day 0 and Day 17 provided a long-term picture. The final comparison, between both experimental groups on Day 0 and Day 2, provided genes involved in short-term temperature response, regardless of direction.

Table 1. Differential expression comparisons made and the number of differentially-expressed contigs to each transcriptome.

Temp. Regime	**Comparison**	**Variable**	**DE Contigs (Complete)**	**DE Contigs (*C. bairdi*)**	**DE Contigs (*Alveolata*)**
Elevated	Day 0 vs. Day 2	Temp.	367	1721	4
Decreased	Day 0 vs. Day 2	Temp.	2033	7	0
Decreased	Day 0 vs. Day 17	Temp.	213	4	0
Decreased	Day 0 vs. Day 2+17	Temp.	389	14	0
Control	Day 0 vs. Day 2	Time	7103	78	0
Control	Day 0 vs. Day 17	Time	4764	473	7
Decreased and Elevated	Day 0 vs. Day 2	Temp.	1113	192	0

C. bairdi

Temperature

To determine the influence of acute temperature change on gene expression in *C. bairdi,* comparisons of gene expression were made within each treatment group prior to, and two days after, the initiation of temperature changes. Within the elevated-temperature treatment group, 1721 contigs were identified as differentially expressed (padj < 0.05) (**Table 1**). Of these, 1473 were expressed at higher levels after the increase from 7.5°C to 10°C. Within the decreased-temperature treatment group, 7 contigs were identified as differentially expressed (padj < 0.05), all of which were expressed at higher levels after the decrease in temperature from 7.5°C to 4°C.

Time

To examine host gene expression changes as the infection develops, gene expression within the control temperature treatment group on Day 0 was compared to expression on Day 17. A total of 473 contigs were differentially expressed (padj < 0.05) (**Table 1)**. Of these, 251 were expressed on higher levels on Day 17. To determine when the changes in expression occurred, each of these groups were compared to libraries from Day 2 from the same crab. Between the first two days, there were 78 differentially expressed contigs, while the subsequent 15 days had 473 differentially expressed contigs. Functional enrichment was then examined, but no substantial enrichment in gene ontology terms was found.

Hematodinium sp.

Temperature

To examine the impact of acute temperature change on gene expression in *Hematodinium*, the same comparisons were made with libraries aligned to the Alveolata transcriptome. Within the elevated-temperature treatment group, four contigs were identified as differentially expressed. Three of these — two (P85200 & O23717) proteasome subunits, and mitochondrial membrane ATP synthase (Q06056) — were matched to the UniProtKB/Swiss-Prot database. Over the same timeframe, no contigs were identified as differentially expressed within the decreased-temperature treatment group.

Time

An examination of change in *Hematodinium* expression as the infection develops was also performed by comparing expression in the control temperature treatment group between Day 0 and Day 17. A total of 7 contigs were identified as differentially expressed, and all were expressed at higher levels by the end of the experiment. When matched to the

UniProtKB/Swiss-Prot database, the protein coding gene C16orf89 (Q6UX73) and a serine protease (P52717) were identified.

Significant changes in functional enrichment were observed between Day 0 and Day 17 (**Figure 2)**. Expression decreased with time in several RNA-related processes, along with ribosomal assembly and cellular component assembly. Simultaneously, expression increased in microtubule-based processes, developmental processes, and movement of cell or subcellular components.

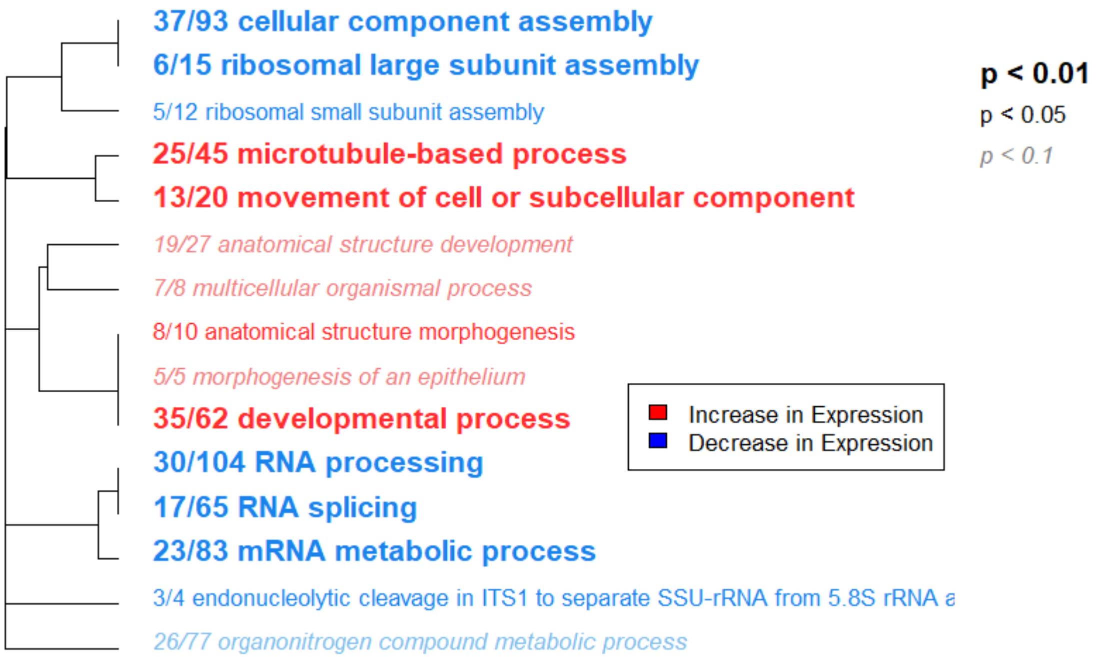

Figure 2. Functional enrichment of Gene Ontology (GO) Biological Process terms of parasite control temperature treatment group expression between Day 0 and Day 17 of the experiment. Tree represents hierarchical clustering based on shared genes. GO terms with zero branch length between them have gene lists in which one is a subset of the other. Text size corresponds to adjusted p-value and text color indicates the direction of regulation. Red corresponds to upregulation while blue indicates downregulation. Numbers indicate the fraction of genes with that GO term with absolute log2 fold change greater than 1.

1.3.4 *Clustering by Expression Patterns*

C. bairdi

WGCNA was used to cluster genes into modules and identify their correlation with experimental variables, along with their correlation to individual crabs. Modules were named with a color to identify them. Modules with a correlation greater than ±0.5 to a single crab were not examined further, as association to a variable was likely due to expression in that individual. Two modules, black and brown, were found to be significantly linked to temperature response (**Figure 3)**. The black module was more expressed at decreased temperatures than control temperatures ($p < 0.0008$), and also more expressed at elevated than non-elevated temperatures ($p = 0.05$). The brown module had lower expression at elevated temperatures when compared to decreased temperatures ($p = 0.02$), or all temperatures ($p = 0.03$) These modules were examined for GO enrichment, but no significant enrichment was found in either.

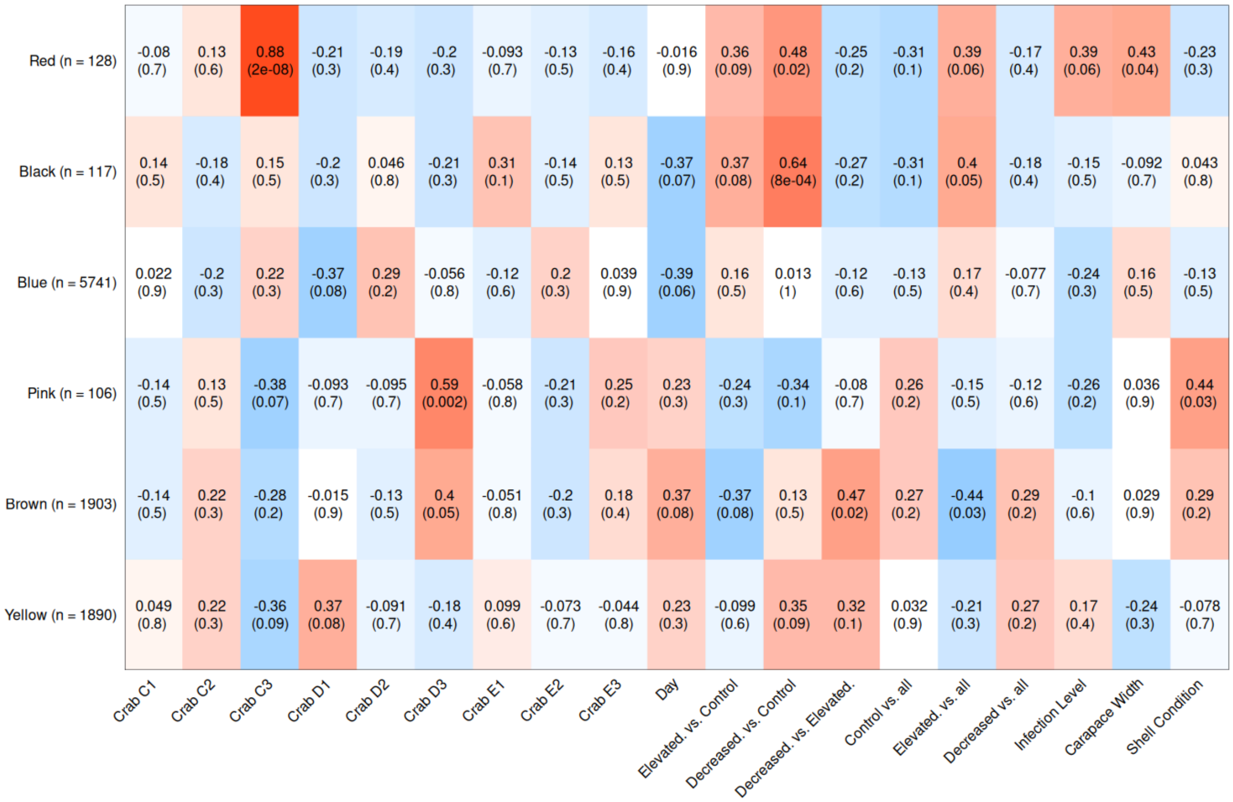

	Crab C1	Crab C2	Crab C3	Crab D1	Crab D2	Crab D3	Crab E1	Crab E2	Crab E3	Day	Elevated. vs. Control	Decreased. vs. Control	Decreased. vs. Elevated.	Control vs. all	Elevated. vs. all	Decreased vs. all	Infection Level	Carapace Width	Shell Condition
Red (n = 128)	-0.08 (0.7)	0.13 (0.6)	0.88 (2e-08)	-0.21 (0.3)	-0.19 (0.4)	-0.2 (0.3)	-0.093 (0.7)	-0.13 (0.5)	-0.16 (0.4)	-0.016 (0.9)	0.36 (0.09)	0.48 (0.02)	-0.25 (0.2)	-0.31 (0.1)	0.39 (0.06)	-0.17 (0.4)	0.39 (0.06)	0.43 (0.04)	-0.23 (0.3)
Black (n = 117)	0.14 (0.5)	-0.18 (0.4)	0.15 (0.5)	-0.2 (0.3)	0.046 (0.8)	-0.21 (0.3)	0.31 (0.1)	-0.14 (0.5)	0.13 (0.5)	-0.37 (0.07)	0.37 (0.08)	0.64 (8e-04)	-0.27 (0.2)	-0.31 (0.1)	0.4 (0.05)	-0.18 (0.4)	-0.15 (0.5)	-0.092 (0.7)	0.043 (0.8)
Blue (n = 5741)	0.022 (0.9)	-0.2 (0.3)	0.22 (0.3)	-0.37 (0.08)	0.29 (0.2)	-0.056 (0.8)	-0.12 (0.6)	0.2 (0.3)	0.039 (0.9)	-0.39 (0.06)	0.16 (0.5)	0.013 (1)	-0.12 (0.6)	-0.13 (0.5)	0.17 (0.4)	-0.077 (0.7)	-0.24 (0.3)	0.16 (0.5)	-0.13 (0.5)
Pink (n = 106)	-0.14 (0.5)	0.13 (0.5)	-0.38 (0.07)	-0.093 (0.7)	-0.095 (0.7)	0.59 (0.002)	-0.058 (0.8)	-0.21 (0.3)	0.25 (0.2)	0.23 (0.3)	-0.24 (0.3)	-0.34 (0.1)	-0.08 (0.7)	0.26 (0.2)	-0.15 (0.5)	-0.12 (0.6)	-0.26 (0.2)	0.036 (0.9)	0.44 (0.03)
Brown (n = 1903)	-0.14 (0.5)	0.22 (0.3)	-0.28 (0.2)	-0.015 (0.9)	-0.13 (0.5)	0.4 (0.05)	-0.051 (0.8)	-0.2 (0.3)	0.18 (0.4)	0.37 (0.08)	-0.37 (0.08)	0.13 (0.5)	0.47 (0.02)	0.27 (0.2)	-0.44 (0.03)	0.29 (0.2)	-0.1 (0.6)	0.029 (0.9)	0.29 (0.2)
Yellow (n = 1890)	0.049 (0.8)	0.22 (0.3)	-0.36 (0.09)	0.37 (0.08)	-0.091 (0.7)	-0.18 (0.4)	0.099 (0.6)	-0.073 (0.7)	-0.044 (0.8)	0.23 (0.3)	-0.099 (0.6)	0.35 (0.09)	0.32 (0.1)	0.032 (0.9)	-0.21 (0.3)	0.27 (0.2)	0.17 (0.4)	-0.24 (0.3)	-0.078 (0.7)

Figure 3. Heatmap of C. bairdi gene expression clusters and variables. X-axis shows variables, y-axis shows module name and the number of genes that make up the module. Each cell in the heatmap contains the correlation between the module and the variable, with the relevant p-value underneath. Cell color corresponds to correlation value, with positive correlations in red, neutral correlations in white, and negative correlations in blue.

To examine how host expression varied with change in *Hematodinium* infection over the course of the experiment, the analysis was repeated excluding samples from crabs that died prior to final sample collection. The same procedure was followed. Modules with significant correlations to variables other than change in *Hematodinium* infection were discarded, as the previous analysis was more apt for examining them. Expression in the red module (**Figure 4**) was significantly correlated to change in *Hematodinium* infection (p = 0.04). This module was examined for GO enrichment, but no significant enrichment was found

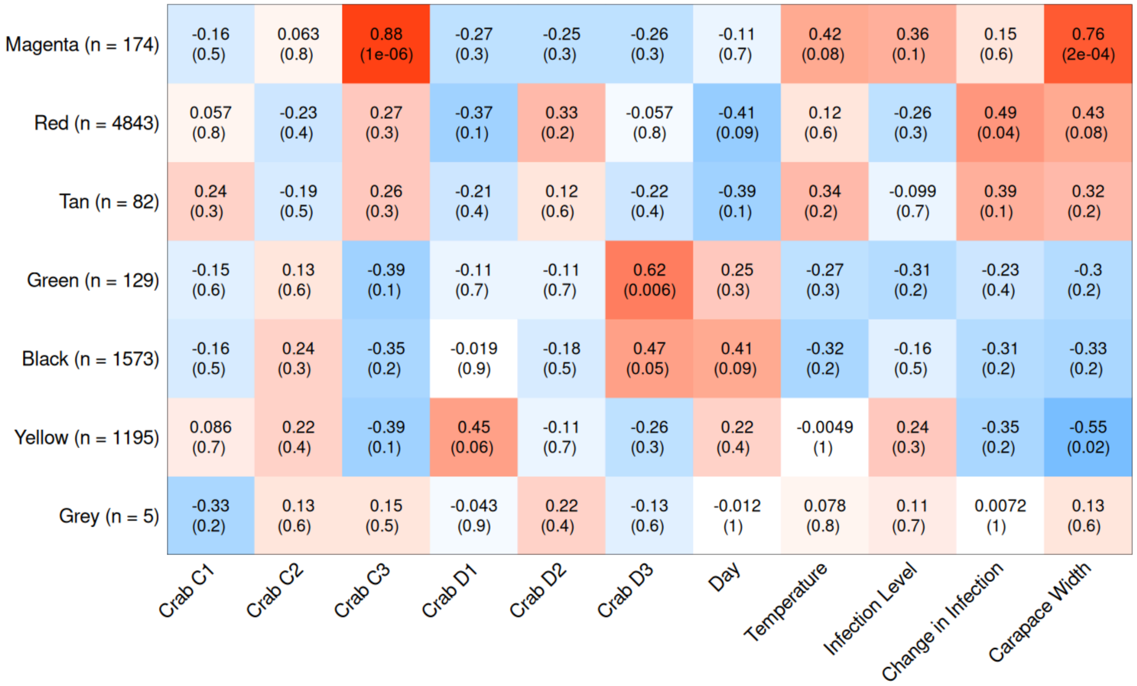

	Crab C1	Crab C2	Crab C3	Crab D1	Crab D2	Crab D3	Day	Temperature	Infection Level	Change in Infection	Carapace Width
Magenta (n = 174)	-0.16 (0.5)	0.063 (0.8)	0.88 (1e-06)	-0.27 (0.3)	-0.25 (0.3)	-0.26 (0.3)	-0.11 (0.7)	0.42 (0.08)	0.36 (0.1)	0.15 (0.6)	0.76 (2e-04)
Red (n = 4843)	0.057 (0.8)	-0.23 (0.4)	0.27 (0.3)	-0.37 (0.1)	0.33 (0.2)	-0.057 (0.8)	-0.41 (0.09)	0.12 (0.6)	-0.26 (0.3)	0.49 (0.04)	0.43 (0.08)
Tan (n = 82)	0.24 (0.3)	-0.19 (0.5)	0.26 (0.3)	-0.21 (0.4)	0.12 (0.6)	-0.22 (0.4)	-0.39 (0.1)	0.34 (0.2)	-0.099 (0.7)	0.39 (0.1)	0.32 (0.2)
Green (n = 129)	-0.15 (0.6)	0.13 (0.6)	-0.39 (0.1)	-0.11 (0.7)	-0.11 (0.7)	0.62 (0.006)	0.25 (0.3)	-0.27 (0.3)	-0.31 (0.2)	-0.23 (0.4)	-0.3 (0.2)
Black (n = 1573)	-0.16 (0.5)	0.24 (0.3)	-0.35 (0.2)	-0.019 (0.9)	-0.18 (0.5)	0.47 (0.05)	0.41 (0.09)	-0.32 (0.2)	-0.16 (0.5)	-0.31 (0.2)	-0.33 (0.2)
Yellow (n = 1195)	0.086 (0.7)	0.22 (0.4)	-0.39 (0.1)	0.45 (0.06)	-0.11 (0.7)	-0.26 (0.3)	0.22 (0.4)	-0.0049 (1)	0.24 (0.3)	-0.35 (0.2)	-0.55 (0.02)
Grey (n = 5)	-0.33 (0.2)	0.13 (0.6)	0.15 (0.5)	-0.043 (0.9)	0.22 (0.4)	-0.13 (0.6)	-0.012 (1)	0.078 (0.8)	0.11 (0.7)	0.0072 (1)	0.13 (0.6)

Figure 4. Heatmap of *C. bairdi* gene expression clusters and variables using only crabs who survived the full experiment. X-axis shows variables, y-axis shows module name and the number of genes that make up the module. Each cell in the heatmap contains the correlation between the module and the variable, with the relevant p-value underneath. Cell color corresponds to correlation value, with positive correlations in red, neutral correlations in white, and negative correlations in blue.

Hematodinium

The same procedure was followed for genes matching the Alveolata transcriptome. The pink module was found to decrease in expression over time (p = 0.03), while the brown module was found to be less expressed in heavily-infected crabs (p = 0.02) (**Figure 5**).

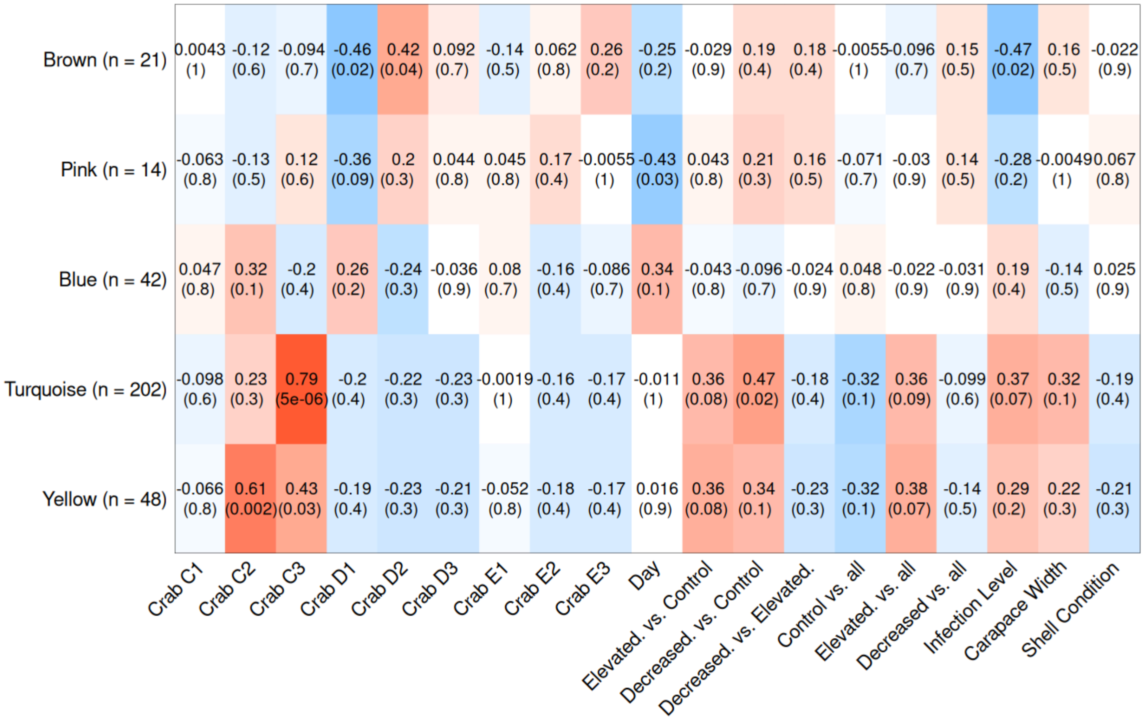

	Crab C1	Crab C2	Crab C3	Crab D1	Crab D2	Crab D3	Crab E1	Crab E2	Crab E3	Day	Elevated. vs. Control	Decreased. vs. Control	Decreased. vs. Elevated.	Control vs. all	Elevated. vs. all	Decreased vs. all	Infection Level	Carapace Width	Shell Condition
Brown (n = 21)	0.0043 (1)	-0.12 (0.6)	-0.094 (0.7)	-0.46 (0.02)	0.42 (0.04)	0.092 (0.7)	-0.14 (0.5)	0.062 (0.8)	0.26 (0.2)	-0.25 (0.2)	-0.029 (0.9)	0.19 (0.4)	0.18 (0.4)	-0.0055 (1)	-0.096 (0.7)	0.15 (0.5)	-0.47 (0.02)	0.16 (0.5)	-0.022 (0.9)
Pink (n = 14)	-0.063 (0.8)	-0.13 (0.5)	0.12 (0.6)	-0.36 (0.09)	0.2 (0.3)	0.044 (0.8)	0.045 (0.8)	0.17 (0.4)	-0.0055 (1)	-0.43 (0.03)	0.043 (0.8)	0.21 (0.3)	0.16 (0.5)	-0.071 (0.7)	-0.03 (0.9)	0.14 (0.5)	-0.28 (0.2)	-0.0049 (1)	0.067 (0.8)
Blue (n = 42)	0.047 (0.8)	0.32 (0.1)	-0.2 (0.4)	0.26 (0.2)	-0.24 (0.3)	-0.036 (0.9)	0.08 (0.7)	-0.16 (0.4)	-0.086 (0.7)	0.34 (0.1)	-0.043 (0.8)	-0.096 (0.7)	-0.024 (0.9)	0.048 (0.8)	-0.022 (0.9)	-0.031 (0.9)	0.19 (0.4)	-0.14 (0.5)	0.025 (0.9)
Turquoise (n = 202)	-0.098 (0.6)	0.23 (0.3)	0.79 (5e-06)	-0.2 (0.4)	-0.22 (0.3)	-0.23 (0.3)	-0.0019 (1)	-0.16 (0.4)	-0.17 (0.4)	-0.011 (1)	0.36 (0.08)	0.47 (0.02)	-0.18 (0.4)	-0.32 (0.1)	0.36 (0.09)	-0.099 (0.6)	0.37 (0.07)	0.32 (0.1)	-0.19 (0.4)
Yellow (n = 48)	-0.066 (0.8)	0.61 (0.002)	0.43 (0.03)	-0.19 (0.4)	-0.23 (0.3)	-0.21 (0.3)	-0.052 (0.8)	-0.18 (0.4)	-0.17 (0.4)	0.016 (0.9)	0.36 (0.08)	0.34 (0.1)	-0.23 (0.3)	-0.32 (0.1)	0.38 (0.07)	-0.14 (0.5)	0.29 (0.2)	0.22 (0.3)	-0.21 (0.3)

Figure 5. Heatmap of parasite gene expression clusters and experimental variables. X-axis shows variables, y-axis shows module name and the number of genes that make up the module. Each cell in the heatmap contains the correlation between the module and the variable, with the relevant p-value underneath. Cell color corresponds to correlation value, with positive correlations in red, neutral correlations in white, and negative correlations in blue.

The pink and brown modules were then examined for gene enrichment. Within the pink module, two pathways were enriched - negative regulation of biological processes (padj = 0.025) and cellular macromolecule catabolic processes (padj = 1 x 10^{-15}). The brown module had numerous enriched pathways, including cytokinesis, vacuole organization, and translational elongation (**Figure 6**).

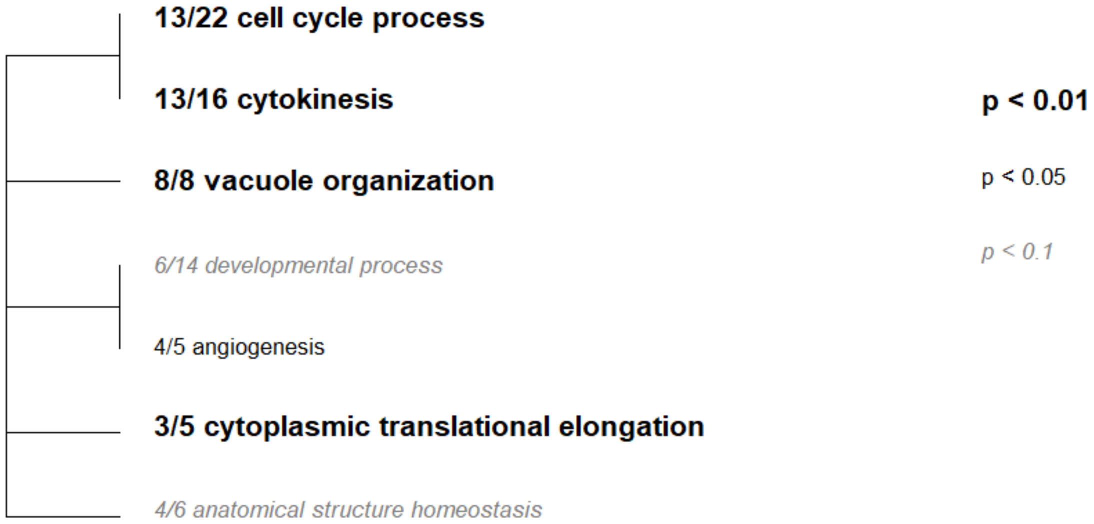

Figure 6. Functional enrichment of GO Biological Process terms within libraries aligned to the parasite transcriptome and clustered into the brown module. Tree represents hierarchical clustering based on shared genes. GO terms with zero branch length between them have gene lists in which one is a subset of the other. Numbers indicate the fraction of genes with that GO term with absolute log2 fold change greater than 1.

1.4 DISCUSSION

1.4.1 *Transcriptome Description*

We provide a *C. bairdi* transcriptome, along with the first transcriptome for any *Hematodinium* species. We also produce the first transcriptional description of a crustacean parasitized by a dinoflagellate, providing valuable insight into the function of a host-parasite system. BUSCO scores indicate that transcriptome completeness was 73.8% for *C. bairdi* and 26.5% for *Hematodinium*.

1.4.2 *Immune Description*

C. bairdi

Of the 49 immune genes observed within the *C. bairdi* transcriptome, over 20% (n = 11) were members of the cathepsin family. Seven of those code for cathepsin or procathepsin L. In multiple crustaceans, cathepsin L has been shown to be upregulated in response to pathogen exposure (Li et al. 2010) (Dai et al. 2017), indicating that further research on *C. bairdi* cathepsins may prove fruitful for uncovering the consequences of *Hematodinium* infection. Furthermore, cathepsin C, which plays an important role in crustacean immunoregulatory function (Liu et al. 2020) was also observed within the transcriptome. Several genes associated with the IMD pathway were observed, including several MAPKs, Relish, IκK, and NFIL3.

Hematodinium

Four genes within the parasite transcriptome were linked to immune function, three of which were papain-family proteases. This provides an intriguing indication of the mechanism by which *Hematodinium* proliferates within the host. For species in the parasitic phylum Apicomplexa, papain-family proteases have been identified as having important roles in cell invasion (Que et al. 2002), including blood cell degradation (Pandey et al. 2005) and cell egress (Verma et al. 2016). Previous studies have found that *Hematodinium* primarily proliferates within the hemolymph of the host (Wheeler et al. 2007), but the exact mechanism of that proliferation has been undetermined. This provides an intriguing indication that papain-family proteases may play important roles in infecting and multiplying within hosts.

1.4.3 *Differential Expression*

C. bairdi

Our pairwise comparison of gene expression within treatment groups identified 1721 contigs as differentially-expressed between control and elevated temperatures. Of these, 86% increased in expression following a temperature rise. This likely indicates that short-term heat exposure represents a substantial metabolic increase or stress response. Previous studies found no increase in growth rate for juvenile male *C. bairdi* raised at 6°C and 9°C (Paul & Paul 2001), suggesting that this increase in expression is largely a stress response. Since very few contigs were differentially expressed when exposed to a decrease in temperature (n = 7), this provides evidence that for infected *C. bairdi*, short-term temperature increases are much more physiologically stressful than short-term temperature decreases within the range of temperatures examined. Given the increase in frequency and severity of marine heat waves throughout much of the range of *C. bairdi* (Carvalho et al. 2021, Di Lorenzo & Mantua 2016), this indicates the substantial portion of wild *C. bairdi* populations that are infected by *Hematodinium* may experience a considerable increase in energetic costs.

The increase in temperature significantly altered expression of numerous stress-related genes. These include cytochrome p450, which is involved in detoxification in crustaceans (Steele et al. 2018), glutathione peroxidase, an enzyme that protects against oxidative stress (Cheng et al. 2020), and PAK2, which stimulates cell survival and growth (Qiu et al. 2017). Additionally, many genes with altered expression patterns were involved with both stress response and the immune system. Three chitinase genes were differentially expressed at elevated temperatures, along with two serine protease inhibitors. Studies in other crab species have shown these genes to be involved in responding to both physiological stress and bacterial infection (Zhou et al. 2018, Bao et al. 2019).

Interestingly, C-type lectin, which is a key component of the innate immune system (Zhu et al. 2016), decreased significantly in expression both after an increase in temperatures and over the 17-day course of the experiment in crabs within the control temperature treatment group. The same pattern was observed in cathepsin L, another important protein involved in the crab immune system (Li et al. 2010), and in several genes related to ubiquitin, which is involved in muscle atrophy (Koenders et al. 2002). This overlap is also seen more broadly — of the 151 identified genes that were differentially expressed between the start and end of the experiment within the control temperature treatment group, 48 were also differentially expressed within the elevated-temperature treatment group following the two-day increase in temperature. For all 48, the change in expression occurred in the same direction. The changes within the control temperature treatment group show how host expression changes as *Hematodinium* infection develops over the 17-day period. Since many of the same expression patterns were observed after only two days at elevated temperatures, this indicates that warming temperatures may speed the development of the infection. As mortality rates for *Chionoecetes* spp. infected by *Hematodinium* are remarkably high (Shields et al. 2005), heat waves could cause large mortality events.

Hematodinium

Within the control temperature treatment group, over the course of the experiment RNA processing and splicing decreased significantly, as did cellular component assembly and mRNA metabolic processes. Meanwhile, microtubule-based processes and developmental processes both increased in expression significantly (**Figure 2**).

Our clustering-based analysis of expression in all crabs also located a module of genes linked to day, with significant enrichment of cellular macromolecule catabolic processes within the module. This enrichment is possibly due to changes in dominant life stages for *Hematodinium* sp. infections. *Hematodinium* has a notoriously complex life cycle (Appleton & Vickerman 1997), with a number of different stages developing within a single host. Since we eliminated all modules predominantly linked to a single crab, this indicates that the potential change in life stage occurred within multiple hosts. Though we are unable to identify those life stages without histology samples, this provides evidence that gene expression may vary substantially between stages, and indicates that RNA sequencing may be an excellent tool for such a diagnostic

CHAPTER 2

2.1 INTRODUCTION

Tanner crab (*Chionoecetes bairdi*) is a marine decapod common to the waters of the North Pacific from Oregon to the Bering Sea (Jadamec et al. 1999). They are abundant along the continental shelf of much of Alaska, and support a valuable commercial fishery (Punt et al. 2016). They are also closely related to the snow crab (*C. opilio*), and commonly produce fertile hybrids where their ranges overlap (Urban et al. 2002). The Bering Sea *C. opilio* fishery has historically been one of the most lucrative fisheries in the United States (Divine et al. 2019), but recently experienced a dramatic and unexpected population crash (Szuwalski et al. 2023).

Both *C. bairdi* and *C. opilio* are infected by *Hematodinium* sp., a parasitic dinoflagellate that, along with other members of its genus, infect over 50 crustacean species around the globe. *Hematodinium* sp. multiplies within the hemolymph and tissues of its hosts, depleting the number of circulating hemocytes and damaging numerous vital organs such as the heart, gills, and hepatopancreas. As the parasite continues to multiply, the host experiences respiratory dysfunction and severe tissue damage, causing lethargy and then death (Wheeler et al. 2007). Transmission is assumed to be waterborne and to occur directly between hosts, as heavily-infected hosts release large numbers of dinospores into the water column (Li et al. 2021). However, the dynamics of transmission are still poorly understood and have proved difficult to unravel. Though the relationship between infection and temperature is uncertain, infection rates in boreal hosts tend to peak in summer (Li et al. 2021), indicating a potential link to climate change.

Hematodinium sp. was first observed in the North Pacific in 1985 - though it may have been present long before - when the southeastern Alaska *C. bairdi* fishery noticed some crabs had a distinctly bitter flavor, along with milky hemolymph and an unusually pink, opaque carapace (Meyers et al. 1987)This combination of symptoms, which came to be called Bitter Crab Syndrome (BCS), was found to be characteristic of late-stage infections. While low-level *Hematodinium* sp. infections cannot be diagnosed without microscopy or genetic sequencing, visual observation can detect BCS with relatively high accuracy (Jadamec 1999). Subsequent research then uncovered a link between BCS and shell condition. Since *C. bairdi* undergoes a terminal molt, terminally-molted crabs see a general deterioration of their shells over time due to natural wear and tear (Tamone et al. 2007). Shell condition is thus used as a proxy for age, as well as time since terminal molt. Crabs with older shells are substantially less likely to display symptoms of BCS, indicating individuals are more prone to infection during or soon after molt (Eaton et al. 1991).

Since its initial observation in 1985, *Hematodinium* sp. has become one of the most common parasites of *C. bairdi* in southeastern Alaska. The region is marked by numerous fjords and bays. This complicates the disease dynamics substantially, with spatially close areas often having different infection rates. Over an eight-year study, nearly 70% of *C. bairdi* assessed in the Port Frederick area were positive for BCS, while at Icy Bay - under 30 miles away - only 4% were positive (Bednarski et al. 2011). Given *C. bairdi* is in a state of panmixia throughout its range (Johnson et al. 2019), infection rates are uncorrelated with host density, and the pattern is still observed even when only examining mature males (Bednarski et al. 2011), these consistent differences in infection rates are unlikely to be caused by differences in hosts. Instead, environmental and parasite-specific variables are likely responsible.

Previous research on factors correlated with *Hematodinium* spp. infection rates have found a number of intriguing associations. Several hosts have displayed seasonal cycles of infection rates, though with substantial variance in peak timing (Davies et al. 2019, Eaton et al. 1991, Smith et al. 2015). In some hosts, molting has also been linked to infection rates, perhaps due to the soft, permeable cuticle of freshly-molted crabs rendering them vulnerable to infection (Shields et al. 2005), which, since smaller individuals molt more frequently, can result in higher infection rates at smaller sizes (Lycett et al. 2019). Several hosts have also demonstrated higher infection rates in females than in males (Stentiford et al. 2001, Lycett et al. 2019). In *Chionoecetes*, the relationship of sex and size to infection remains unclear, with studies finding conflicting results (Eaton et al. 1991, Pestal et al. 2003, Shields et al. 2005).

As *C. bairdi* supports a valuable commercial fishery and *Hematodinium* sp. infections are thought to be fatal (Shields et al. 2005), it is important to understand what renders individuals vulnerable to infection. With that aim, we used a multidecadal dataset, collected using consistent methodology, to uncover physiological and environmental variables correlated with *Hematodinium* sp. infection.

2.2 METHODS

2.2.1 *Survey Design*

Annual pot surveys were conducted by the Alaska Department of Fish and Game (ADF&G) from 2005 to 2019. Two surveys were conducted each year. The red king crab survey (RKC survey) was carried out from June to August and was focused on the red king crab (*Paralithodes camtschaticus*) stock, though large numbers of *C. bairdi* were caught as well. The

C. bairdi survey was carried out from September to October, and was focused on the *C. bairdi* stock.

Both surveys were conducted in numerous survey areas within Southeast Alaska (**Figure 7**). With the exception of Holkham Bay and Juneau, there was no overlap in survey areas between the *C. bairdi* survey and the RKC survey.

Each survey area was divided into density strata using a Neyman allocation based on the variance of crab density estimates over a three-year period (Rebert et al. 2019, Stratman et al. 2019). The number of pots for the survey area, determined based on logistical feasibility, were then divided among density strata. Precise pot locations were randomly assigned within each stratum using Geospatial Modeling Environment (Bayer 2004) with a minimum distance of 0.1 nautical miles between pots. If a pot location was not possible due to gear conflicts or other issues, a preselected pot location was used. Pots were set from 12:00 to 18:00 and pulled from 07:00 to 13:00. Soak times ranged from 18 to 20 hours for the RKC survey and 16 to 20 hours for the *C. bairdi* survey. The survey used conical top-loading commercial crab pots with an 88-inch diameter and no escape rings. Frozen herring or a mix of frozen herring and pink salmon was used as bait. A temperature logger was attached to each pot, with temperature readings taken at one-hour intervals for all surveys except the 2005 *C. bairdi* survey, which had temperature readings taken every 3 hours and 30 minutes.

For each *C. bairdi* captured, sex and shell condition were determined and the specimen was measured for carapace width (CW) using standard ADF&G codes and protocols (Jacamec et al. 1999). The presence of bitter crab syndrome (BCS) and infection with black mat fungus (*Trichomaris invadens*), along with the presence of other pathogens, was noted when present, as were any missing legs or carapace damage. Female crabs were classified for maturity and measured for clutch fullness. If present, the condition of any eggs was noted. A subset of male crabs were measured for right chela height, as the ratio of carapace width to chela height indicates crab maturity.

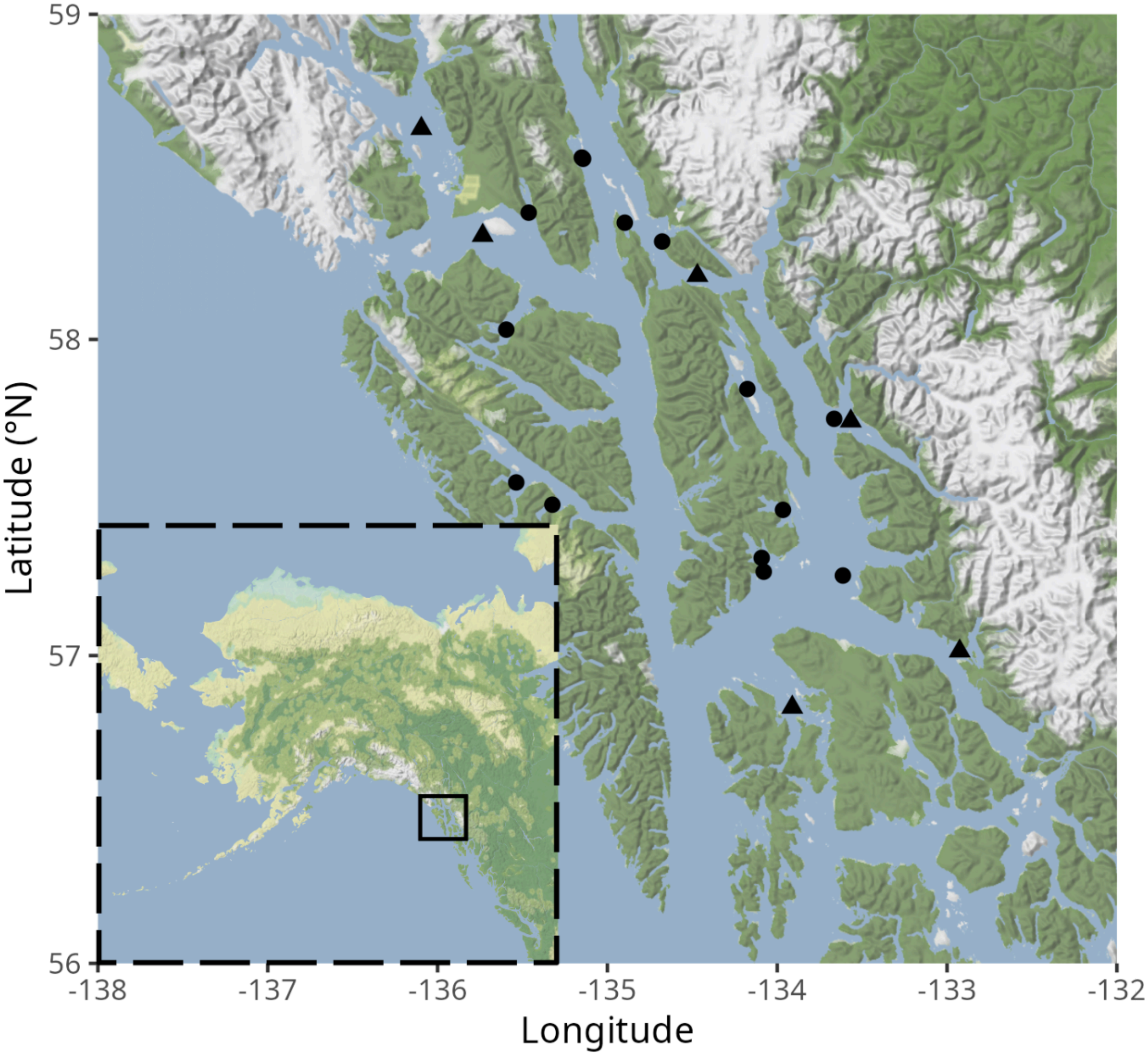

Figure 7. Survey locations, as determined by average pot latitude and longitude. Circles represent red king crab survey locations, while triangles represent Tanner crab survey locations.

2.2.2 *Data Analysis and Modeling*

Temperature data were obtained by cross-referencing pot set and pot retrieval times with data from the temperature loggers. Temperature for the pot deployment was determined by excluding readings taken within one hour of pot setting or retrieval to account for discrepancies in timekeeping, and then averaging the remaining readings. Pot deployments with a temperature variance of over 3°C were discarded, as this indicates the pot was likely not deployed for part of the timeframe. All deployments with an average temperature over 9°C were manually checked by cross-referencing the logger data files with NOAA sea surface temperature for that day and area (NOAA National Data Buoy Center 1971), as well as an examination of the trends in the logger data files. Apparent data entry errors were discarded. Temperature readings were then averaged for all pots at the site for that year, producing the temperatures generally experienced by the crab in its environment.

Apparent data entry errors, incomplete entries, and irrelevant variables were eliminated, leaving a total of 151,313 measurements. To identify factors affecting BCS prevalence, generalized linear mixed models (GLMMs) were fitted using the R package glmmTMP (Brooks et al. 2017). Predictors of BCS prevalence were shell condition (light, new, old, very old), temperature (°C), carapace width (mm), injuries (present/absent), sex (male/female), latitude, presence of Black Mat, and depth (meters). Year and site were used as random effects, as baseline rates of infection differ consistently between sites and across years. Continuous predictors were scaled, and categorical predictors were converted to factors. Shell condition was specified to be an ordered factor. Julian day was not used, as it covaried with temperature.

As *C. bairdi* displays pronounced sexual dimorphism, with males being much larger than females (Jadamec et al. 1999), carapace width was scaled separately for males and females. Collinearity of predictors was assessed using VIFs, with no variables having high collinearity (>5). Models were examined to check model assumptions, overdispersion, and goodness of fit.

Models were weighted based on AICc, and a weighted average was taken of all models with a weight of 0.01 or greater.

$$Infection_{i,j,k} \sim Binomial(\mu_{i,j,k})$$
$$E(Infection_{i,j,k}) = \mu_{i,j,k}$$
$$log\frac{(\mu_{i,j,k})}{(1-\mu_{i,j,k})} = ShellCondition_{i,j,k} + Temperature_{i,j} + CarapaceWidth_{i,j,k} + BlackMat_{i,j,k} + \\ + Sex_{i,j,k} + Latitude_{i,j,k} + Depth_{i,j,k} + Year_{i} + Site_{j}$$
$$Year_{i} \sim N(0, \sigma^2)$$
$$Site_{j} \sim N(0, \sigma^2)$$

Equation 1. The full model, in which Infection$_{i,j,k}$ is the k^{th} crab in year i at site j, Year$_i$ and Site$_j$ are the random effects, which are assumed to be normally distributed with mean 0 and variance σ^2

To determine whether certain measured sex-specific factors were associated with infection, two more models were created following the same protocol and incorporating sex-specific measurements.

$$Infection_{i,j,k} \sim Binomial(\mu_{i,j,k})$$
$$E(Infection_{i,j,k}) = \mu_{i,j,k}$$
$$log\frac{(\mu_{i,j,k})}{(1-\mu_{i,j,k})} = ShellCondition_{i,j,k} + Temperature_{i,j} + CarapaceWidth_{i,j,k} + BlackMat_{i,j,k} + \\ + Latitude_{i,j,k} + Depth_{i,j,k} + ClutchFullness_{i,j,k} + EggDev_{i,j,k} + Year_{i} + Site_{j}$$
$$Year_{i} \sim N(0, \sigma^2)$$
$$Site_{j} \sim N(0, \sigma^2)$$

Equation 2. The female-specific model modified the full model by incorporating clutch fullness (percent) and the amount of egg development (juvenile, barren, uneyed, eyed) as predictors, while dropping sex as a predictor since only female measurements were used. A total of 24,726 measurements were used for the female-specific model.

$$Infection_{i,j,k} \sim Binomial(\mu_{i,j,k})$$
$$E(Infection_{i,j,k}) = \mu_{i,j,k}$$
$$log\frac{(\mu_{i,j,k})}{(1-\mu_{i,j,k})} = ShellCondition_{i,j,k} + Temperature_{i,j} + CarapaceWidth_{i,j,k} + BlackMat_{i,j,k} + \\ + Sex_{i,j,k} + Latitude_{i,j,k} + Depth_{i,j,k} + Year_{i} + Site_{j}$$
$$Year_{i} \sim N(0, \sigma^2)$$
$$Site_{j} \sim N(0, \sigma^2)$$

Equation 3. The male-specific model took the full model and added maturity status (immature/mature) as calculated by the ratio of chela height to carapace width (Tamone et al. 2007), while dropping sex as only males were examined. A total of 23,461 measurements were used for this model.

2.3 RESULTS

2.3.1 *General Model*

Of the 8 predictor variables examined, 6 were significant ($p < 0.05$) (**Figure 8**). New-shell crabs were more likely than old-shell crabs to show signs of BCS ($p < 0.0001$). Carapace width was positively associated with infection ($p < 0.0001$), while depth was negatively correlated ($p < 0.0001$). Female crabs were more prone to infection than were males ($p < 0.0001$). Crabs infected with T. invadens were less likely to display signs of BCS ($p < 0.0001$), though with a relatively high standard error (0.18) as only 4% of individuals were infected by *T. invadens*. There was a weak relationship to temperature, with warmer sites showing higher rates of infection ($p = 0.012$). No relationship was observed with leg condition ($p = 0.32$) or latitude ($p = 0.71$).

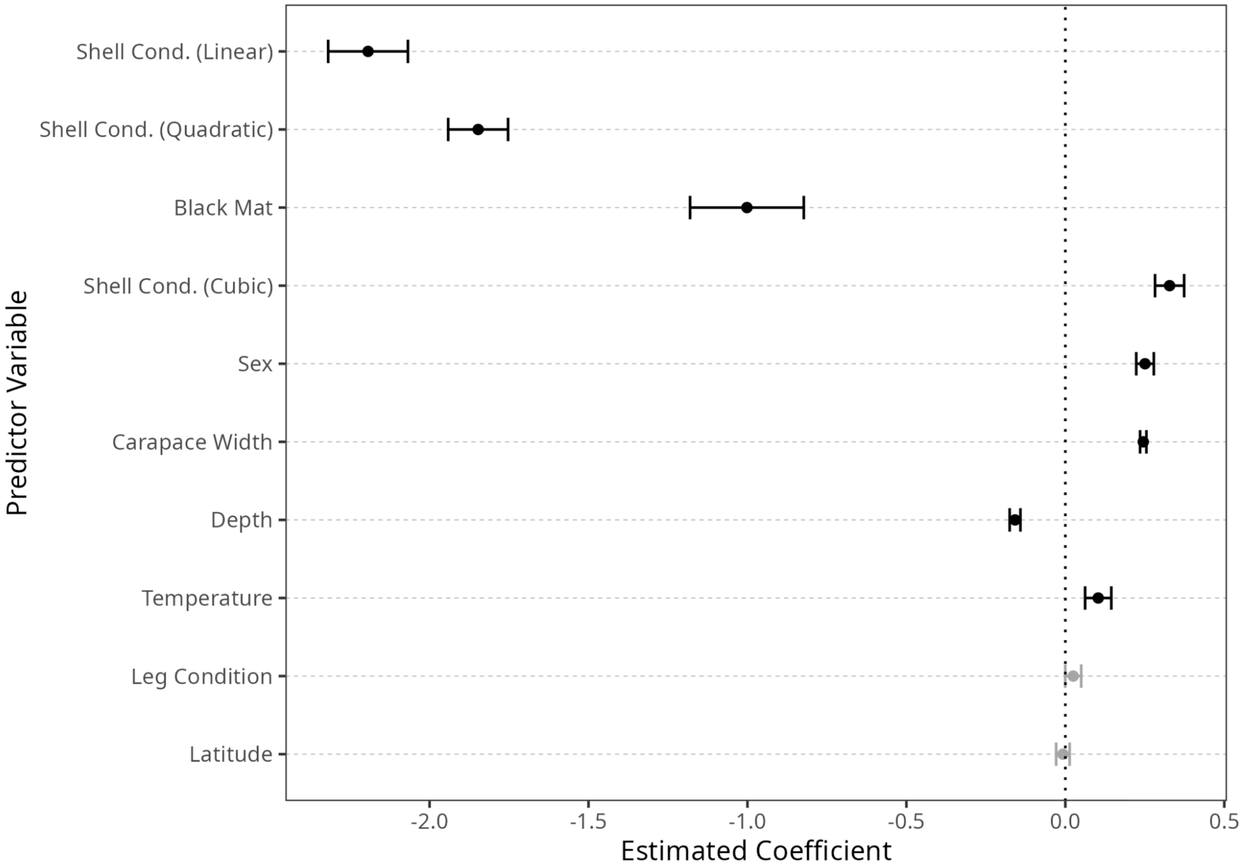

Figure 8. Estimated coefficients of each predictor variable in the averaged general model. Variables are listed in descending order of absolute value of estimated coefficient. As shell condition is an ordered factor, it has three associated coefficients. Error bars represent adjusted standard error. Coefficients in black are significant, while coefficients in gray are not.

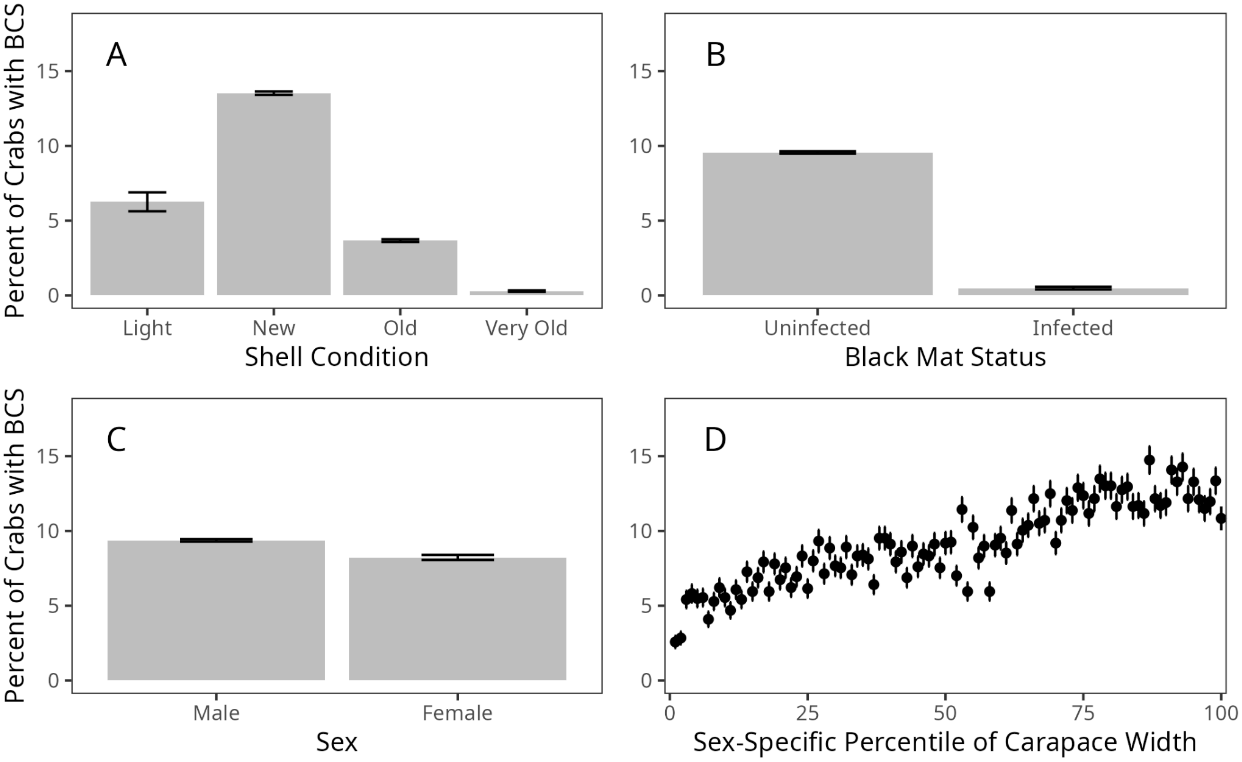

Figure 9. Relationships present in the raw data between BCS status and the four predictor variables with the largest coefficients in the general model. Error bars represent standard error. Y-axis scaling is constant between all graphs. As *C. bairdi* is sexually dimorphic with substantially larger adult males, each sex separately had carapace width measurements binned by percentile, and the BCS rate of each percentile was then visualized in Figure 9D. This mimics how carapace width was treated in the GLMMs.

2.3.2 *Female-Specific Model*

Generally, variables examined in the female-specific model (**Figure 10)** displayed the same relationships as those in the general model. The exceptions are temperature (p = 0.25) and infection with *T. invadens* (p = 0.18), neither of which was significant in this model. Of the new sex-specific predictors, immature females had higher rates of infection than mature females (p = 0.028), while females with a higher clutch fullness had lower rates of infection (p < 0.0001). The raw data, however, appears to reveal a normal distribution, with highest infection rates at medium clutch fullness (**Figure 11B**). However, it appears that this is due to the rarity of infected crabs with high clutch fullness (**Figure 11C)**.

2.3.3 *Male-Specific Model*

The predictors in the male-specific model (**Figure 10)** generally followed the same patterns of significance as the general model, though, as with the female-specific model, both temperature ($p = 0.41$) and infection with *T. invadens* ($p = 0.97$) were not significant in this model. Additionally, though not significant in the general model, the presence of injuries was positively correlated with infection status in the male-specific model ($p = 0.0009$). Maturity status was significant ($p < 0.0001$), with higher infection rates among immature males than among mature males (**Figure 11D**).

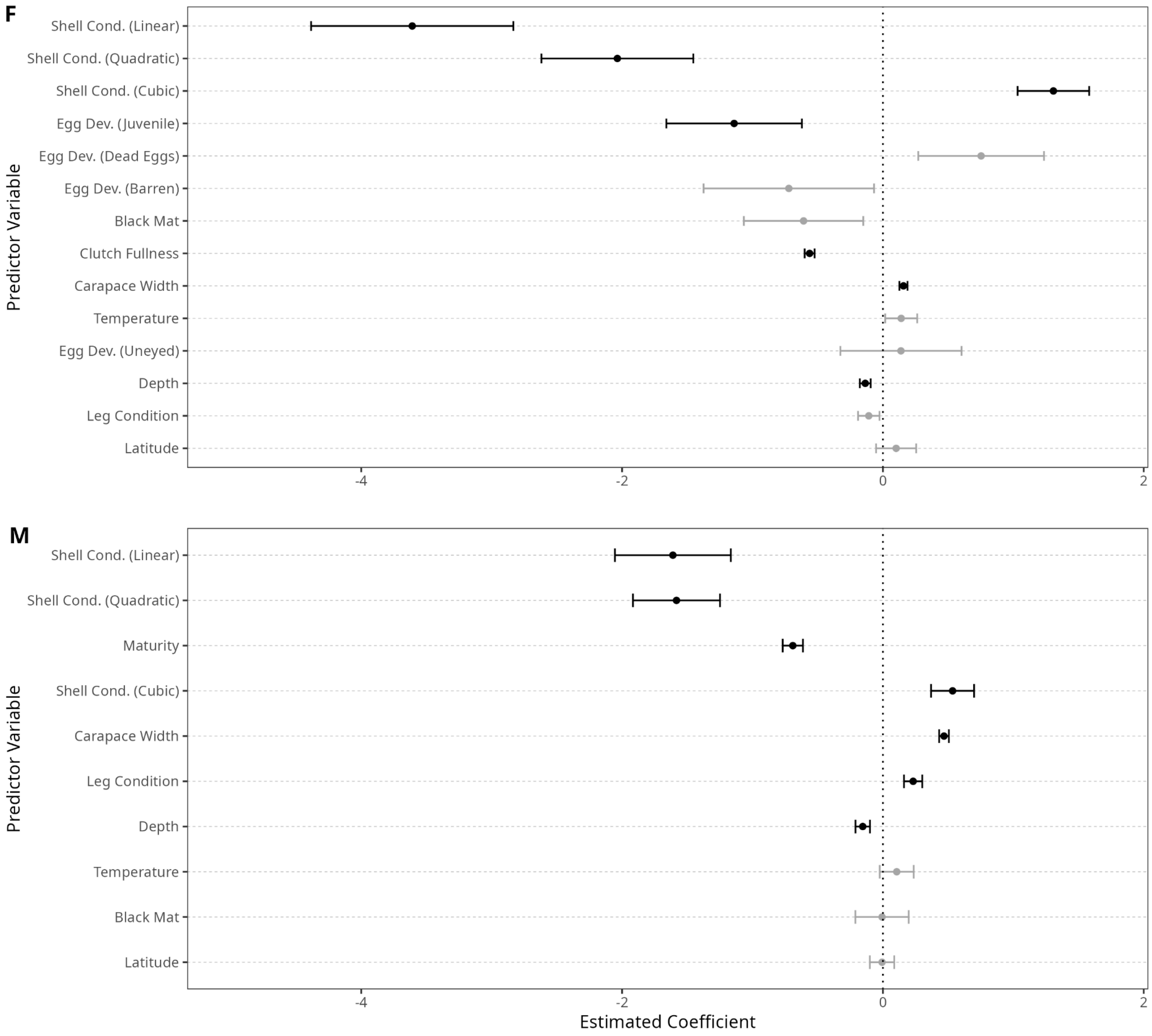

Figure 10. Estimated coefficients of each predictor in the sex-specific averaged models. F corresponds to the female model, M to the male model. Predictors are ranked in order of descending absolute value for each, and x-axis is shared for both. Shell condition and egg development (in the female model) have several associated coefficients, as they are factors. Error bars represent standard error. Coefficients in black are significant, while coefficients in grey are not.

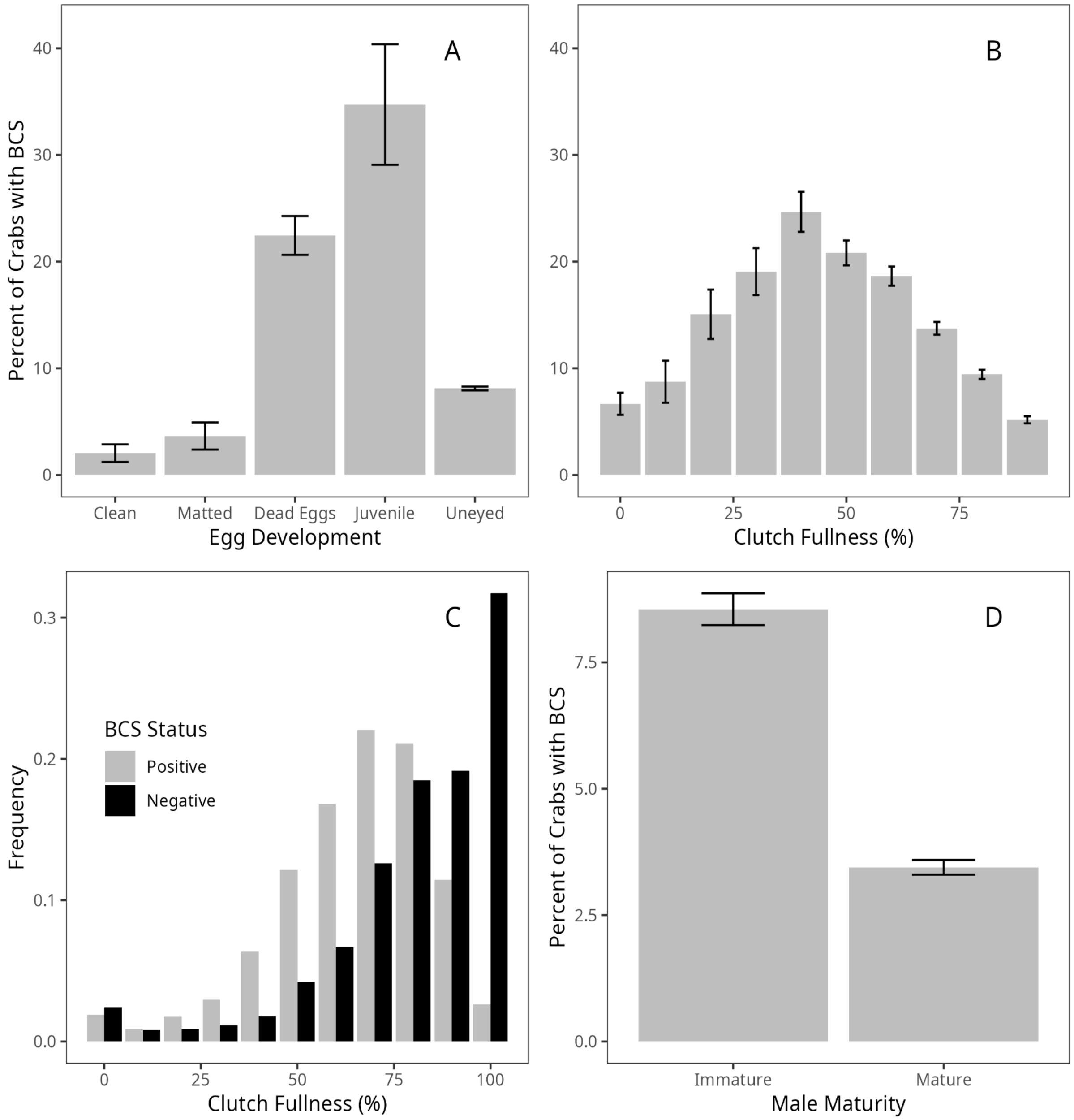

Figure 11. Relationships present in the raw data between BCS status and the significant sex-specific predictors in the female-specific model (A-C) and male-specific model (D). When present, error bars represent standard error. Only categories with over 50 measurements are graphed. Figure 11B shows the infection rates at each level of clutch fullness, while Figure 11C shows overlapping histograms of clutch fullness for both BCS-positive and negative crabs. Y-axes are not held constant between figures, with the exception of 11A and 11B.

2.4 DISCUSSION

We found that infection status was related to a number of biological variables, namely carapace width, sex, maturity status, clutch status (for females), and time since molt. Depth was the only environmental variable with a consistent relationship to infection status.

Within all models, the coefficient with the highest absolute value was, by a substantial portion, shell condition. This finding agrees with existing research, as numerous studies have found that recently-molted *C. bairdi* are more prone to infection by *Hematodinium* sp., potentially due to the soft, permeable nature of the shell shortly after molting (Eaton et al. 1991, Imamura & Woodby 1994). Crabs with a shell condition of “Light”, which corresponds to 2-8 weeks post-molt (Jadamec et al. 1999) are less likely than new-shell crabs, but more likely than old-shell crabs, to display signs of BCS (**Figure 8, Figure 9A**). From this, it is apparent that the minimum time between infection and visible symptoms of BCS is, for some individuals, less than eight weeks.

The second-highest absolute value within the full model was sex (0.250). Interestingly, when examining the raw data, males were more likely to be infected than females (**Figure 9C)**, while the model found that females were more likely to be infected than males (**Figure 8**). Previous research on this subject has been contradictory. Within a population of the closely-related *C. opilio* in the Canadian Maritimes, females were more likely than males to be infected by *Hematodinium* sp. (Pestal et al. 2003), while earlier studies of Alaskan *C. bairdi* found no relationship between sex and infection rates (Eaton et al. 1991), or found males to be more likely to be infected than females (Bednarski et al. 2011). However, both Alaskan studies dealt with smaller sample sizes, and both only examined sex without investigating the importance of other variables, such as location and shell condition. It appears that by examining many variables simultaneously, including treating year and site as random effects, we were able to uncover a more accurate relationship between sex and infection rate.

Carapace width was also influential in all models, with both general and sex-specific models finding larger crabs to be more likely to be infected. Again, previous studies have found conflicting results, with no relationship found in Alaskan *C. bairdi* (Eaton et al. 1991), while a relationship was found in a larger trawl study on Atlantic *C. opilio* (Shields et al. 2005). Interestingly, while this latter study found similar results for female crabs, with larger crabs more prone to infection, it found that the likelihood of infection decreased with size in male crabs. This diverges from our study, which found larger crabs to have a higher rate of infection. The *C. opilio* study used trawls to obtain crabs, and thus captured crabs were unable to enter a pot. If size classes are differentially impacted by the weakness and lethargy of late-stage infection, our findings could be explained by gear selectivity. Differences in data analysis could also be responsible. While this study differentiated between mature and immature males in our male-specific model, the *C. opilio* study did not. Given that our study also found immature males to be infected at higher rates, this could explain the overall negative relationship they observed between carapace width and infection rates. Finally, different disease dynamics could be taking place between Atlantic *C. opilio* and Pacific *C. bairdi*. From a physiological perspective, immune response is increasingly being seen as a trade-off. In mosquitoes, an immune challenge reduces egg production (Ahmed et al. 2002), and in crickets, larger, faster-growing individuals are slower to encapsulate abiotic material (Rantala et al. 2005). It is possible that larger individuals are investing proportionally more energy in growth and molting, resulting in a weaker immune system. However, future research is necessary to unravel the causes behind the higher infection rates in larger crabs.

The female-specific model found clutch fullness to be a significant predictor (**Figure 10)**, and examination of the raw data revealed infection rates peaked at medium clutch fullness, with low rates at either extreme (**Figure 11B**). No previous research can be found examining the relationship between *Hematodinium* sp. infection and clutch fullness for any host species. Given that under 3% of infected females had full clutches, compared to over 30% of uninfected females (**Figure 11C**), it seems likely that infection reduces host fecundity, as has been observed in numerous other crustacean host-parasite systems (Bollache et al. 2002, Kuris 1990). However, high-fecundity females may be healthier, with more robust immune systems, and thus more resistant to infection, as in other systems infection does not reduce fecundity (Bhaduri et al. 2002, Öndes et al. 2016). Regardless, the relationship uncovered here adds nuance to our understanding of the dynamics of the *Hematodinium* sp.- *C. bairdi* host-parasite relationship and highlights likely impacts of *Hematodinium* sp. on host reproduction.

While coinfection with *T. invadens* was significant in the full model ($p < 0.0001$), its standard error was also quite high (0.18). In both the male-specific and female-specific model, coinfection was not found to be significant, likely due to the reduced sample size and consequently lower statistical power. Though it is possible that *T. invadens* reduces the likelihood of coinfection by *Hematodinium* sp., as competition between parasites has been observed in numerous host-parasite systems (Wood & Johnson 2015), it is also possible these findings are due to the methodology of the survey. Both *T. invadens* and *Hematodinium* sp. are visually diagnosed by an abnormal shell appearance, and the black fungal mat of *T. invadens* infection could obscure the characteristic "milky" shell of *Hematodinium* sp. infection.

Therefore, while the strong negative relationship between the two parasites is intriguing, and competition between the two parasites is a possibility, additional research is necessary to determine whether *Hematodinium* sp. and *T. invadens* are in competition.

Given its long development time and the difficulty of experimentally infecting crabs, understanding this system has proven difficult. The use of GLMMs on a multi-decadal survey data set has provided essential insights into the relationship of biological and environmental variables on the likelihood of *Hematodinium* sp. infection. For the first time in North Pacific *Chionoecetes*, a relationship has been shown between *Hematodinium* sp. infection and sex, along with carapace width and clutch fullness. Additionally, *T. invadens* and *Hematodinium* sp. were found to be potentially competing for hosts, though future research is necessary to determine whether this apparent dynamic is due to the impact of *T. invadens* on host appearance. In summation, this study provides important insights into the dynamics of this host-parasite system. Given the recent unexpected collapses of Alaskan *Chionoecetes* populations, (Szuwalski et al. 2023), incorporating these findings into our understanding of population dynamics is critical. Furthermore, determining whether these same relationships are observed in other hosts could illuminate our understanding of how *Hematodinium* operates, and, as *Hematodinium* continues to regularly appear in new hosts (Hong et al. 2023, Li et al. 2021, Ryazonova et al. 2021), could be of critical importance to understanding the disease dynamics of *Hematodinium* in other crustacean species.

REFERENCES

Ahmed, A. M., S. L. Baggott, R. Maingon, and H. Hurd. 2002. "The Costs of Mounting an Immune Response Are Reflected in the Reproductive Fitness of the Mosquito *Anopheles Gambiae*." *Oikos* 97 (3): 371–77.

Alimin, Ade Wahyul Fajri, Nor Asma Husna Yusoff, Ince Ayu Khairana Kadriah, Hilal Anshary, Farizan Abdullah, Nurhidayah Jabir, Endang Susianingsih, and Marina Hassan. 2023. "Parasitic Dinoflagellate Hematodinium in Marine Decapod Crustaceans: A Review on Current Knowledge and Future Perspectives." *Parasitology Research* 123 (1): 49.

Andrews, S. 2010. "FastQC: A Quality Control Tool for High Throughput Sequence Data." https://www.bioinformatics.babraham.ac.uk/projects/fastqc/.

Appleton, P. L., and K. Vickerman. 1998. "In Vitro Cultivation and Developmental Cycle in Culture of a Parasitic Dinoflagellate (Hematodinium Sp.) Associated with Mortality of the Norway Lobster (Nephrops Norvegicus) in British Waters." *Parasitology* 116 (Pt 2) (February): 115–30.

Bao, Jie, Yue-Nan Xing, Hong-Bo Jiang, and Xiao-Dong Li. 2019. "Identification of Immune-Related Genes in Gills of Chinese Mitten Crabs (Eriocheir Sinensis) during Adaptation to Air Exposure Stress." *Fish & Shellfish Immunology* 84 (January): 885–93.

Bednarski, J., C. E. Siddon, G. H. Bishop, and J. F. Morado. 2011. "Overview of Bitter Crab Disease in Tanner Crabs, Chionoecetes Bairdi, in Southeast Alaska from 2001 to 2008." In *Biology and Management of Exploited Crab Populations under Climate Change*. Alaska Sea Grant, University of Alaska Fairbanks. https://doi.org/10.4027/bmecpcc.2010.07.

Bhaduri, Ritindra N., Taiga J. Yamaguchi, Kimberly Munguia, Royal K. Sandhu, and Victoria R. Coffey. 2022. "Impact of the Acanthocephalan Parasite *Profilicollis Altmani* on the Fecundity of Its Crustacean Intermediate Host, the Pacific Mole Crab, *Emerita Analoga*." *Invertebrate Biology: A Quarterly Journal of the American Microscopical Society and the Division of Invertebrate Zoology/ASZ* 141 (1). https://doi.org/10.1111/ivb.12362.

Bollache, L., T. Rigaud, and F. Cézilly. 2002. "Effects of Two Acanthocephalan Parasites on the Fecundity and Pairing Status of Female Gammarus Pulex (Crustacea: Amphipoda)." *Journal of Invertebrate Pathology* 79 (2): 102–10.

Bray, Nicolas L., Harold Pimentel, Páll Melsted, and Lior Pachter. 2016. "Near-Optimal Probabilistic RNA-Seq Quantification." *Nature Biotechnology* 34 (5): 525–27.

Brooks, Molliee, Kasper Kristensen, Koenj van Benthem, Arni Magnusson, Casperw Berg, Anders Nielsen, Hansj Skaug, Martin Mächler, and Benjaminm Bolker. 2017.

“GlmmTMB Balances Speed and Flexibility among Packages for Zero-Inflated Generalized Linear Mixed Modeling.” *The R Journal* 9 (2): 378.

Buchfink, Benjamin, Chao Xie, and Daniel H. Huson. 2015. “Fast and Sensitive Protein Alignment Using DIAMOND.” *Nature Methods* 12 (1): 59–60.

Carvalho, K. S., T. E. Smith, and S. Wang. 2021. “Bering Sea Marine Heatwaves: Patterns, Trends and Connections with the Arctic.” *Journal of Hydrology* 600 (September): 126462.

Chen, Shifu, Yanqing Zhou, Yaru Chen, and Jia Gu. 2018. “Fastp: An Ultra-Fast All-in-One FASTQ Preprocessor.” *Bioinformatics* 34 (17): i884–90.

Cheng, Chang-Hong, Hong-Ling Ma, Yi-Qin Deng, Juan Feng, Xiao-Long Chen, and Zhi-Xun Guo. 2020. “Glutathione Peroxidase 3 in the Mud Crab Scylla Paramamosain: Characterization and Regulation under Nitrite Stress.” *Comparative Biochemistry and Physiology. Toxicology & Pharmacology: CBP* 229 (March): 108673.

Cheung, William W. L., and Thomas L. Frölicher. 2020. “Marine Heatwaves Exacerbate Climate Change Impacts for Fisheries in the Northeast Pacific.” *Scientific Reports* 10 (1): 6678.

Crandall, Grace, Pamela C. Jensen, Samuel J. White, and Steven Roberts. 2022. “Characterization of the Gene Repertoire and Environmentally Driven Expression Patterns in Tanner Crab (Chionoecetes Bairdi).” *Marine Biotechnology* 24 (1): 216–25.

Crosson, Lisa M. 2011. “Development and Validation of a Quantitative Real-Time Polymerase Chain Reaction (qPCR) Assay to Assess the Impact of Hematodinium, a Parasitic Dinoflagellate, on Tanner Crab Populations in Alaska.” University of Washington.

Dai, Li-Shang, Sheng-Hui Chu, Xiao-Min Yu, and Yan-Yan Li. 2017. “A Role of Cathepsin L Gene in Innate Immune Response of Crayfish (Procambarus Clarkii).” *Fish & Shellfish Immunology* 71 (December): 246–54.

Davies, Charlotte E., Frederico M. Batista, Sophie H. Malkin, Jessica E. Thomas, Charlotte C. Bryan, Peter Crocombe, Christopher J. Coates, and Andrew F. Rowley. 2019. “Spatial and Temporal Disease Dynamics of the Parasite Hematodinium Sp. in Shore Crabs, Carcinus Maenas.” *Parasites & Vectors* 12 (1): 472.

Di Lorenzo, Emanuele, and Nathan Mantua. 2016. “Multi-Year Persistence of the 2014/15 North Pacific Marine Heatwave.” *Nature Climate Change* 6 (11): 1042–47.

Divine, Lauren M., Franz J. Mueter, Gordon H. Kruse, Bodil A. Bluhm, Stephen C. Jewett, and Katrin Iken. 2019. “New Estimates of Weight-at-Size, Maturity-at-Size, Fecundity, and Biomass of Snow Crab, Chionoecetes Opilio, in the Arctic Ocean off Alaska.” *Fisheries Research* 218 (October): 246–58.

Ewels, Philip, Måns Magnusson, Sverker Lundin, and Max Käller. 2016. “MultiQC: Summarize Analysis Results for Multiple Tools and Samples in a Single Report.” *Bioinformatics* 32 (19): 3047–48.

Gong, Miao, Guosi Xie, Hailiang Wang, Xinshu Li, Ang Li, Xiaoyuan Wan, Jingxian Huang, Chengyin Shi, Qingli Zhang, and Jie Huang. 2023. “Hematodinium Perezi Naturally Infects Asian Brush-Clawed Crab (Hemigrapsus Takanoi).” *Journal of Fish Diseases* 46 (1): 67–74.

Grabherr, Manfred G., Brian J. Haas, Moran Yassour, Joshua Z. Levin, Dawn A. Thompson, Ido Amit, Xian Adiconis, et al. 2011. “Full-Length Transcriptome Assembly from RNA-Seq Data without a Reference Genome.” *Nature Biotechnology* 29 (7): 644–52.

Haas, Brian J., Alexie Papanicolaou, Moran Yassour, Manfred Grabherr, Philip D. Blood, Joshua Bowden, Matthew Brian Couger, et al. 2013. “De Novo Transcript Sequence Reconstruction from RNA-Seq Using the Trinity Platform for Reference Generation and Analysis.” *Nature Protocols* 8 (8): 1494–1512.

Hamilton, K. M., P. W. Shaw, and D. Morritt. 2009. “Prevalence and Seasonality of Hematodinium (Alveolata: Syndinea) in a Scottish Crustacean Community.” *ICES Journal of Marine Science: Journal Du Conseil* 66 (9): 1837–45.

Heller-Shipley, Madison A., William T. Stockhausen, Benjamin J. Daly, André E. Punt, and Scott E. Goodman. 2021. “Should Harvest Control Rules for Male-Only Fisheries Include Reproductive Buffers? A Bering Sea Tanner Crab (Chionoecetes Bairdi) Case Study.” *Fisheries Research* 243 (November): 106049.

Hl, Beyer. 2004. “Hawth’s Analysis Tools for ArcGIS.” *Http://Www. Spatialecology. Com/Htools*. https://cir.nii.ac.jp/crid/1570009750911540736.

Holdo, Ricardo M., Anthony R. E. Sinclair, Andrew P. Dobson, Kristine L. Metzger, Benjamin M. Bolker, Mark E. Ritchie, and Robert D. Holt. 2009. “A Disease-Mediated Trophic Cascade in the Serengeti and Its Implications for Ecosystem C.” *PLoS Biology* 7 (9): e1000210.

Howard Hughes Medical Institute. n.d. “Hmmscan: Search Sequence(s) against a Profile Database:” hmmer.org.

Huson, Daniel H., Sina Beier, Isabell Flade, Anna Górska, Mohamed El-Hadidi, Suparna Mitra, Hans-Joachim Ruscheweyh, and Rewati Tappu. 2016. “MEGAN Community Edition - Interactive Exploration and Analysis of Large-Scale Microbiome Sequencing Data.” *PLoS Computational Biology* 12 (6): e1004957.

Jacamec, Luke S., William E. Donaldson, Paula Cullenberg}. 1999. *Biological Field Techniques for Chionoecetes Crabs*. University of Alaska Sea Grant College Program.

Jensen, Pamela C., Katy Califf, Vanessa Lowe, Lorenz Hauser, and J. Frank Morado. 2010. "Molecular Detection of Hematodinium Sp. in Northeast Pacific Chionoecetes Spp. and Evidence of Two Species in the Northern Hemisphere." *Diseases of Aquatic Organisms* 89 (2): 155–66.

Johnson, Genevieve M. 2019. "Genetic Diversity and Population Genetic Structure of Tanner Crab Chionoecetes Bairdi in Alaskan Waters." Edited by J. Andres Lopez. Ann Arbor, United States: University of Alaska Fairbanks. https://www.proquest.com/dissertations-theses/genetic-diversity-population-structure-tanner/docview/2217079968/se-2.

Ken Imamura And. 1994. "Marketability Testing of Tanner Crab (Chionoecetes Bairdi) Infected by a Hematodinium-like Dinoflagellate, the Probable Cause of Bitter Crab Syndrome." IJ94-01. Alaska Department of Fish and Game.

Koenders, Annette, Xiaoli Yu, Ernest S. Chang, and Donald L. Mykles. 2002. "Ubiquitin and Actin Expression in Claw Muscles of Land Crab, Gecarcinus Lateralis, and American Lobster, Homarus Americanus: Differential Expression of Ubiquitin in Two Slow Muscle Fiber Types during Molt-Induced Atrophy." *The Journal of Experimental Zoology* 292 (7): 618–32.

Kuris, Armand. 1990. *Crustacean Egg Production*. Taylor & Francis Group.

Langfelder, Peter, and Steve Horvath. 2008. "WGCNA: An R Package for Weighted Correlation Network Analysis." *BMC Bioinformatics* 9 (December): 559.

Li, Caiwen, Meng Li, and Qian Huang. 2021. "The Parasitic Dinoflagellate Hematodinium Infects Marine Crustaceans." *Marine Life Science & Technology*, January. https://doi.org/10.1007/s42995-020-00061-z.

Li, Caiwen, Terrence L. Miller, Hamish J. Small, and Jeffrey D. Shields. 2011. "In Vitro Culture and Developmental Cycle of the Parasitic Dinoflagellate Hematodinium Sp. from the Blue Crab Callinectes Sapidus." *Parasitology* 138 (14): 1924–34.

Li, Caiwen, Jeffrey D. Shields, Terrence L. Miller, Hamish J. Small, Katrina M. Pagenkopp, and Kimberly S. Reece. 2010. "Detection and Quantification of the Free-Living Stage of the Parasitic Dinoflagellate Hematodinium Sp. in Laboratory and Environmental Samples." *Harmful Algae* 9 (5): 515–21.

Li, Meng, Qian Huang, Xiaoyang Lv, Shuqun Song, and Caiwen Li. 2021. "The Parasitic Dinoflagellate Hematodinium Infects Multiple Crustaceans in the Polyculture Systems of Shandong Province, China." *Journal of Invertebrate Pathology* 178 (January): 107523.

Li, Wei-Wei, Xing-Kun Jin, Lin He, Hui Jiang, Ya-Nan Gong, Yan-Nan Xie, and Qun Wang. 2010. "Molecular Cloning, Characterization, Expression and Activity Analysis of

Cathepsin L in Chinese Mitten Crab, Eriocheir Sinensis.” *Fish & Shellfish Immunology* 29 (6): 1010–18.

Li, Yingdong, Weibin Xu, Xin Li, Hongbo Jiang, Qiuxin She, Zhibin Han, Xiaodong Li, and Qijun Chen. 2018. “Comparative Transcriptome Analysis of Chinese Grass Shrimp (Palaemonetes Sinensis) Infected with Isopod Parasite Tachaea Chinensis.” *Fish & Shellfish Immunology* 82 (November): 153–61.

Lindner, Scott E., Kristian E. Swearingen, Melanie J. Shears, Michael P. Walker, Erin N. Vrana, Kevin J. Hart, Allen M. Minns, Photini Sinnis, Robert L. Moritz, and Stefan H. I. Kappe. 2019. “Transcriptomics and Proteomics Reveal Two Waves of Translational Repression during the Maturation of Malaria Parasite Sporozoites.” *Nature Communications* 10 (1): 4964.

Liu, Qiu-Ning, Saima Kausar, Isma Gul, Hai-Ling Zhou, Muhammad Nadeem Abbas, and Li-Shang Dai. 2020. “The Red Swamp Crayfish, Procambarus Clarkii Cathepsin C, Participates in the Innate Immune Response to the Viral and Bacterial Pathogens.” *Fish & Shellfish Immunology* 100 (May): 436–44.

Love, D. C., S. D. Rice, D. A. Moles, and W. D. Eaton. 1993. “Seasonal Prevalence and Intensity of Bitter Crab Dinoflagellate Infection and Host Mortality in Alaskan Tanner Crabs Chionoeceles Bairdi from Auke Bay, Alaska, USA.” *Diseases of Aquatic Organisms* 15: 1–7.

Love, Michael I., Wolfgang Huber, and Simon Anders. 2014. “Moderated Estimation of Fold Change and Dispersion for RNA-Seq Data with DESeq2.” *Genome Biology* 15 (12): 550.

Lycett, Kristen A., J. Sook Chung, and Joseph S. Pitula. 2018. “The Relationship of Blue Crab (Callinectes Sapidus) Size Class and Molt Stage to Disease Acquisition and Intensity of Hematodinium Perezi Infections.” *PloS One* 13 (2): e0192237.

Martin, Melanie, Aaron D. Blackwell, Michael Gurven, and Hillard Kaplan. 2013. “Make New Friends and Keep the Old? Parasite Coinfection and Comorbidity in Homo Sapiens.” In *Primates, Pathogens, and Evolution*, edited by Jessica F. Brinkworth and Kate Pechenkina, 363–87. New York, NY: Springer New York.

Messick, G. A. 1994. “Hematodinium Perezi Infections in Adult Arid Juvenile Blue Crabs Callinectes Sapidus from Coastal Bays of Maryland and Virginia, USA.” *Diseases of Aquatic Organisms* 19: 77–82.

Meyers, T. R., C. Botelho, T. M. Koeneman, S. Short, and K. Imamura. 1990. “Distribution of Bitter Crab Dinoflagellate Syndrome in Southeast Alaskan Tanner Crabs Chionoecetes Bairdi.” *Diseases of Aquatic Organisms* 9: 37–43.

Meyers, T. R., T. M. Koeneman, C. Botelho, and S. Short. 1987. “Bitter Crab Disease: A Fatal Dinoflagellate Infection and Marketing Problem for Alaskan Tanner Crabs Chionoecetes Bairdi.” *Diseases of Aquatic Organisms* 3 (3): 195–216.

Morado, J. F., E. G. Dawe, D. Mullowney, C. A. Shavey, V. C. Lowe, and R. J. Cawthorn. 2011. “Climate Change and the Worldwide Emergence of Hematodinium-Associated Disease: Is There Evidence for a Relationship?” In *Biology and Management of Exploited Crab Populations under Climate Change*, 153–73. Alaska Sea Grant, University of Alaska Fairbanks.

NOAA National Data Buoy Center. 1971. “Meteorological and Oceanographic Data Collected from the National Data Buoy Center Coastal-Marine Automated Network (C-MAN) and Moored (Weather) Buoys.” NOAA National Centers for Environmental Information (NCEI). https://www.ncei.noaa.gov/archive/accession/NDBC-CMANWx.

Öndes, Fikret, Michel J. Kaiser, Lee G. Murray, and Gabriela Torres. 2016. “Reproductive Ecology, Fecundity, and Elemental Composition of Eggs in Brown Crab Cancer Pagurus in The Isle of Man.” *Journal of Shellfish Research* 35 (2): 539–47.

Pandey, Kailash C., Stephanie X. Wang, Puran S. Sijwali, Anthony L. Lau, James H. McKerrow, and Philip J. Rosenthal. 2005. “The Plasmodium Falciparum Cysteine Protease Falcipain-2 Captures Its Substrate, Hemoglobin, via a Unique Motif.” *Proceedings of the National Academy of Sciences of the United States of America* 102 (26): 9138–43.

Paul, A. J., and J. M. Paul. 2001. “Effects of Temperature on Length of Intermolt Periods in Juvenile Male Chionoecetes Bairdi.” *Alaska Fisheries Research Bulletin* 8: 132–34.

Pestal, Gottfried P., David M. Taylor, John M. Hoenig, Jeffrey D. Shields, and Roger Pickavance. 2003. “Monitoring the Prevalence of the Parasitic Dinoflagellate Hematodinium Sp. in Snow Crabs Chionoecetes Opilio from Conception Bay, Newfoundland.” *Diseases of Aquatic Organisms* 53 (1): 67–75.

Punt, André E., Robert J. Foy, Michael G. Dalton, W. Christopher Long, and Katherine M. Swiney. 2015. “Effects of Long-Term Exposure to Ocean Acidification Conditions on Future Southern Tanner Crab (Chionoecetes Bairdi) Fisheries Management.” *ICES Journal of Marine Science: Journal Du Conseil* 73 (3): 849–64.

Qiu, Gao-Feng, Liang-Wei Xiong, Zhi-Ke Han, Zhi-Qiang Liu, Jian-Bin Feng, Xu-Gan Wu, Yin-Long Yan, Hong Shen, Long Huang, and Li Chen. 2017. “A Second Generation SNP and SSR Integrated Linkage Map and QTL Mapping for the Chinese Mitten Crab Eriocheir Sinensis.” *Scientific Reports* 7 (January): 39826.

Que, Xuchu, Huân Ngo, Jeffrey Lawton, Mary Gray, Qing Liu, Juan Engel, Linda Brinen, Partho Ghosh, Keith A. Joiner, and Sharon L. Reed. 2002. “The Cathepsin B of Toxoplasma Gondii, Toxopain-1, Is Critical for Parasite Invasion and Rhoptry Protein Processing.” *The Journal of Biological Chemistry* 277 (28): 25791–97.

Rantala, M. J., and D. A. Roff. 2005. “An Analysis of Trade-Offs in Immune Function, Body Size and Development Time in the Mediterranean Field Cricket, Gryllus Bimaculatus.” *Functional Ecology* 19 (2): 323–30.

Ryazanova, T. V., M. G. Eliseikina, and A. D. Kukhlevsky. 2021. “First Detection of Hematodinium Sp. in Spiny King Crab Paralithodes Brevipes, and New Geographic Areas for the Parasite in Tanner Crab Chionoecetes Bairdi, and Red King Crab Paralithodes Camtschaticus.” *Journal of Invertebrate Pathology*, August, 107651.

Shen, Wei, Shuai Le, Yan Li, and Fuquan Hu. 2016. “SeqKit: A Cross-Platform and Ultrafast Toolkit for FASTA/Q File Manipulation.” *PloS One* 11 (10): e0163962.

Shields, Jeffrey D., Juan Pablo Huchin-Mian Huchin-Mian, Pattie A. O’Leary, and Hamish J. Small. 2017. “New Insight into the Transmission Dynamics of the Crustacean Pathogen Hematodinium Perezi (Dinoflagellata) Using a Novel Sentinel Methodology.” *Marine Ecology Progress Series* 573: 73.

Shields, Jeffrey D., David M. Taylor, Paul G. O’Keefe, Eugene Colbourne, and Elaine Hynick. 2007. “Epidemiological Determinants in Outbreaks of Bitter Crab Disease (Hematodinium Sp.) in Snow Crabs Chionoecetes Opilio from Conception Bay, Newfoundland, Canada.” *Diseases of Aquatic Organisms* 77 (1): 61–72.

Shields, Jeffrey D., David M. Taylor, Stephen G. Sutton, Paul G. O’Keefe, Danny W. Ings, and Amanda L. Pardy. 2005. “Epidemiology of Bitter Crab Disease (Hematodinium Sp.) in Snow Crabs Chionoecetes Opilio from Newfoundland, Canada.” *Diseases of Aquatic Organisms* 64 (3): 253–64.

Shipley, Madison A. 2020. “Reproductive Buffers on Exploitation in Male-Only Fisheries: Tanner Crab (Chionoecetes Bairdi) Management Strategy Evaluation Case Study.” Edited by André E. Punt. Ann Arbor, United States: University of Washington. https://www.proquest.com/dissertations-theses/reproductive-buffers-on-exploitation-male-only/docview/2489325022/se-2.

Simão, Felipe A., Robert M. Waterhouse, Panagiotis Ioannidis, Evgenia V. Kriventseva, and Evgeny M. Zdobnov. 2015. “BUSCO: Assessing Genome Assembly and Annotation Completeness with Single-Copy Orthologs.” *Bioinformatics* 31 (19): 3210–12.

Small, Hamish J. 2012. “Advances in Our Understanding of the Global Diversity and Distribution of Hematodinium Spp. - Significant Pathogens of Commercially Exploited Crustaceans.” *Journal of Invertebrate Pathology* 110 (2): 234–46.

Smith, Amanda L., Lucy Hirschle, Claire L. Vogan, and Andrew F. Rowley. 2015. “Parasitization of Juvenile Edible Crabs (Cancer Pagurus) by the Dinoflagellate, Hematodinium Sp.: Pathobiology, Seasonality and Its Potential Effects on Commercial Fisheries.” *Parasitology* 142 (3): 428–38.

Stanke, Mario, Mark Diekhans, Robert Baertsch, and David Haussler. 2008. "Using Native and Syntenically Mapped cDNA Alignments to Improve de Novo Gene Finding." *Bioinformatics* 24 (5): 637–44.

Stanke, Mario, and Stephan Waack. 2003. "Gene Prediction with a Hidden Markov Model and a New Intron Submodel." *Bioinformatics* 19 Suppl 2 (October): ii215-25.

Steele, Alexandra N., Rachelle M. Belanger, and Paul A. Moore. 2018. "Exposure Through Runoff and Ground Water Contamination Differentially Impact Behavior and Physiology of Crustaceans in Fluvial Systems." *Archives of Environmental Contamination and Toxicology* 75 (3): 436–48.

Stentiford, G. D., D. M. Neil, and R. J. A. Atkinson. 2001. "The Relationship of Hematodinium Infection Prevalence in a Scottish Nephrops Norvegicus Population to Season, Moulting and Sex." *ICES Journal of Marine Science: Journal Du Conseil* 58 (4): 814–23.

Stentiford, Grant D., and Jeffrey D. Shields. 2005. "A Review of the Parasitic Dinoflagellates Hematodinium Species and Hematodinium-like Infections in Marine Crustaceans." *Diseases of Aquatic Organisms* 66 (1): 47–70.

Szuwalski, Cody S., Kerim Aydin, Erin J. Fedewa, Brian Garber-Yonts, and Michael A. Litzow. 2023. "The Collapse of Eastern Bering Sea Snow Crab." *Science* 382 (6668): 306–10.

Tompkins, D. M., A. R. White, and M. Boots. 2003. "Ecological Replacement of Native Red Squirrels by Invasive Greys Driven by Disease." *Ecology Letters* 6 (3): 189–96.

Urban, Daniel, Douglas Pengilly, Luke Jadamec, and Susan C. Byersdorfer. 2002. "Testing Carapace Morphology Characteristics for Field Identification of Chionoecetes Hybrids." *Crabs in Coldwater Regions: Biology, Management, and Economics. Fairbanks: University of Alaska*, 97–113.

Verma, Sonia, Rajnikant Dixit, and Kailash C. Pandey. 2016. "Cysteine Proteases: Modes of Activation and Future Prospects as Pharmacological Targets." *Frontiers in Pharmacology* 7 (April): 107.

Wang, Huan, Ce Shi, Mengyao Kong, Changkao Mu, Hongling Wei, and Chunlin Wang. 2018. "Cloning and Expression of a Transcription Factor Activator Protein-1 Member Identified from the Swimming Crab Portunus Trituberculatus." *Cell Stress & Chaperones* 23 (6): 1275–82.

Waterhouse, Robert M., Mathieu Seppey, Felipe A. Simão, Mosè Manni, Panagiotis Ioannidis, Guennadi Klioutchnikov, Evgenia V. Kriventseva, and Evgeny M. Zdobnov. 2018. "BUSCO Applications from Quality Assessments to Gene Prediction and Phylogenomics." *Molecular Biology and Evolution* 35 (3): 543–48.

Wheeler, Kersten, Jeffrey D. Shields, and David M. Taylor. 2007. “Pathology of Hematodinium Infections in Snow Crabs (Chionoecetes Opilio) from Newfoundland, Canada.” *Journal of Invertebrate Pathology* 95 (2): 93–100.

Wood, Chelsea L., and Pieter Tj Johnson. 2015. “A World without Parasites: Exploring the Hidden Ecology of Infection.” *Frontiers in Ecology and the Environment* 13 (8): 425–34.

Wright, Rachel M., Galina V. Aglyamova, Eli Meyer, and Mikhail V. Matz. 2015. “Gene Expression Associated with White Syndromes in a Reef Building Coral, Acropora Hyacinthus.” *BMC Genomics* 16 (May): 371.

Zhang, Runfeng, Fang Liu, Peter Hunt, Congjun Li, Lichun Zhang, Aaron Ingham, and Robert W. Li. 2019. “Transcriptome Analysis Unraveled Potential Mechanisms of Resistance to Haemonchus Contortus Infection in Merino Sheep Populations Bred for Parasite Resistance.” *Veterinary Research* 50 (1): 7.

Zhou, Falin, Kaimin Zhou, Jianhua Huang, Qibin Yang, Song Jiang, Lihua Qiu, Lishi Yang, and Shigui Jiang. 2018. “Characterization and Expression Analysis of a Chitinase Gene (PmChi-5) from Black Tiger Shrimp (Penaeus Monodon) under Pathogens Infection and Ambient Ammonia-N Stress.” *Fish & Shellfish Immunology* 72 (January): 117–23.

Zhou, Yi-Lian, Lan-Zhi Wang, Wen-Bin Gu, Cong Wang, Qi-Hui Zhu, Ze-Peng Liu, Yu-Yin Chen, and Miao-An Shu. 2018. “Identification and Functional Analysis of Immune Deficiency (IMD) from Scylla Paramamosain: The First Evidence of IMD Signaling Pathway Involved in Immune Defense against Bacterial Infection in Crab Species.” *Fish & Shellfish Immunology* 81 (October): 150–60.

Zhu, You-Ting, Xing Zhang, Shi-Chuang Wang, Wei-Wei Li, and Qun Wang. 2016. “Antimicrobial Functions of EsLecH, a C-Type Lectin, via JNK Pathway in the Chinese Mitten Crab, Eriocheir Sinensis.” *Developmental and Comparative Immunology* 61 (August): 225–35.